RSC Advances

ROYAL SOCIETY OF CHEMISTRY

www.rsc.org/advances

Synthesis and inhibitive performance of novel cationic and gemini surfactants on carbon steel corrosion in 0.5 M H_2SO_4 solution

M.A. Hegazy[a,*], A.S. El-Tabei[a], A.H. Bedair[b], M.A. Sadeq[b]

[a]Egyptian Petroleum Research Institute (EPRI), Nasr City, 11727, Cairo, Egypt

[b] Faculty of Science, Al-Azhar University, Chemistry Dept., Nasr City, 11787, Cairo, Egypt

Abstract

Novel cationic and gemini surfactants were synthesized and characterized. The corrosion inhibition efficiency of the synthesized surfactants was studied, on carbon steel in 0.5 M H_2SO_4, by weight loss, potentiodynamic polarization and EIS. The results revealed that both cationic and gemini surfactants were effectively inhibited the corrosion of carbon steel in 0.5 M H_2SO_4. The corrosion inhibition efficiencies obtained were calculated by weight loss and electrochemical experiments. The potentiodynamic polarization studies revealed that the inhibitors acted as mixed-type inhibitors. Thermodynamic parameters of adsorption and kinetic were obtained from weight loss at different temperatures (20–60 ^{o}C). The inhibitors adsorption on carbon steel surface obeyed Langmuir isotherm.

Keywords: Surfactants; Carbon steel; EIS; Weight loss; Polarization; Acid inhibition; Surface properties.

* Corresponding author. Tel.: +20 1002653529; fax: +20 222747433.

E-mail address: mohamed_hgazy@yahoo.com (M.A. Hegazy).

1. Introduction

Carbon steel is the most widely used as a constructional material in many industries due to its excellent mechanical and low cost. It is used in large tonnages in marine applications, chemical processing, petroleum production (refining construction) and metal processing equipment. Acid solutions are widely used in industry, e.g., chemical cleaning, descaling, pickling and oil-well acidizing, which leads to corrosive attack. Therefore, the consumption of inhibitors to reduce corrosion has increased in recent years. The corrosion control by inhibitors is one of the most common effective and economic methods to protect metals in acidic media [1–7]. The majority of the well-known inhibitors are organic compounds containing heteroatom, such as O, N, or S, and multiple bonds, which allow adsorption on the metal surface [8–13].

Gemini surfactants exhibit many unique properties in comparison to single-chained conventional surfactants, so it is reasonable to design and synthesize novel gemini surfactants with different structures and study their effects on the corrosion inhibition of metals. Gemini surfactants become the focus of study in recent years [8,14–16], although numerous corrosion inhibitors have been developed and reported. Gemini surfactants containing heterocyclic ring and their applications in corrosion inhibition of metals are rarely reported.

Schiff bases, the condensation product of an amine and a ketone or aldehyde with general formula of $R_2C=NR$ are well-known organic inhibitors [17,18]. Some research-works revealed that, the inhibition efficiency of the Schiff bases was much greater than that of corresponding amines and aldehydes due to the presence of a -CH=N- group in the molecules [17].

Our goal of this work was directed to synthesize a cationic surfactant ((Z)-1-dodecyl-2-(2-hydroxybenzylideneamino) pyridinium bromide), in addition to, creation of a new type of bis-Schiff base based on gemini cationic surfactant (2,2'-(pentane-1,5-diylidene bis(azan-1-yl-1-ylidene))bis(1-dodecylpyridinium bromide)). The inhibition performance of the novel synthesized cationic and gemini surfactants for carbon steel in acidic medium was investigated using weight loss, potentiodynamic polarization and electrochemical impedance spectroscopy (EIS). The C_{cmc} values of the prepared surfactants were determined by surface tension and conductivity measurements. The surface parameters were calculated by surface tension measurements. The relation between surface properties and the metal corrosion inhibition efficiencies of the prepared surfactants was also discussed.

2. Materials and Experimental Methods

2.1. Materials

2.1.1. Carbon steel specimens

Carbon steel specimens of the following chemical composition (wt. %) were used in the experiment: 0.19% C, 0.05% Si, 0.94% Mn, 0.009% P, 0.004% S, 0.014% Ni, 0.009% Cr, 0.034% Al, 0.016% V, 0.003% Ti, 0.022% Cu, and balance Fe.

A pre-treatment was carried out prior to each experiment, in which specimen surface was mechanically grinded with 340, 400, 600, 800, 1000 and 1200 grades of emery paper, rinsed with bidistilled water, degreased in ethanol and dried at room temperature before use. They were also degreased with acetone and rinsed with distilled water two times and finally dried.**2.2. Synthesis of novel surfactants**

2.2.1. Synthesis of a novel cationic surfactant

A novel cationic surfactant was synthesized through two steps as shown in Fig. 1.

1-Synthesis of (Z)-2-((pyridin-2-ylimino)methyl)phenol

Schiff base reaction between (1.22 g, 0.01 mol) of salicyldehyde and (0.94 g, 0.01 mol) of 2-aminopyridine in ethanol at 70 ^{o}C for 6 h [19] to produce (Z)-2-((pyridin-2-ylimino)methyl)phenol. The mixture was allowed to cool down, then the obtained yellow precipitate was further purified by diethyl ether then recrystallized from ethanol.

2-Synthesis of (Z)-1-dodecyl-2-(2-hydroxybenzylideneamino)pyridinium bromide

Quaternization reaction of (Z)-2-((pyridin-2-ylimino)methyl)phenol (1.98 g, 0.01 mol) and 1-bromododecane (2.49 g, 0.01 mol) in ethanol at 70 ^{o}C for 24 h [20] to produce (Z)-1-dodecyl-2-(2-hydroxybenzylideneamino)pyridinium bromide. The mixture was allowed to cool down. The obtained light yellow precipitate was further purified by diethyl ether then recrystallized from ethanol.

2.2.2. Synthesis of a novel cationic gemini surfactant

A novel cationic gemini surfactant used in this study was synthesized as shown in Fig. 2. This process was carried out in two steps as follow:

1- Synthesis of N,N'-(pentane-1,5-diylidene)dipyridin-2-amine

Schiff base reaction was carried out between (1.00 g, 0.01 mol) of glutaraldehyde and (1.88 g, 0.02 mol) of 2-aminopyridine in ethanol at 70 ^{o}C for 6 h [21] in order to produce N,N'-(pentane-1,5-diylidene)dipyridin-2-amine and a trace of byproduct (N,N'E,N,N'E)-N,N'-((E)-2-((E)-5-(pyridin-2-ylimino)pentylidene)pentane-1,5-diylidene)bis(pyridin-2-amine). The mixture was allowed to cool down. The obtained yellow precipitate was further purified by diethyl ether then recrystallized from ethanol.

2- Synthesis of 2,2'-(pentane-1,5-diylidenebis(azan-1-yl-1-ylidene))bis(1-dodecylpyridinium bromide)

Quaternization reaction of N,N'-(pentane-1,5-diylidene)dipyridin-2-amine (2.52 g, 0.01 mol) and 1-bromododecane (4.98 g, 0.02 mol) in ethanol at 70 ^{o}C for 24 h [22] to produce 2,2'-(pentane-1,5-diylidenebis(azan-1-yl-1-ylidene))bis(1-dodecylpyridinium bromide). The mixture was allowed to cool. The obtained light yellow precipitate was further purified by diethyl ether then recrystallized from ethanol.

The chemical structure of the synthesized compounds was confirmed by elemental analysis, FTIR, ^{1}HNMR and Mass spectroscopy.

2.3 Solutions

The 0.5 M H_2SO_4 was prepared by dilution of analytical grade H_2SO_4 (98 %/wt) with distilled water. The molecular weights of the synthesized cationic and cationic gemini surfactant are 447.45 and 750.66, respectively. The concentration range of used synthesized inhibitors varied from 1×10^{-4} to 5×10^{-2} M for corrosion measurements and from 1×10^{-6} to 1×10^{-2} M for both surface tension and conductivity measurements. Double distilled water was used for preparing test solutions in all measurements.

2.4. Weight loss measurements

The rectangular specimens of carbon steel (7 cm × 3 cm × 0.5 cm) were accurately weighed and then immersed for up to 24 h in a solution containing 0.5 M H_2SO_4 with and without different concentrations of each surfactant. Afterwards, the steel sheets were taken out, rinsed thoroughly with distilled water, dried, and accurately weighed.

2.5. Electrochemical measurements

Polarization experiments were carried out using a conventional three-electrode cell with a platinum counter electrode (CE) and a saturated calomel electrode (SCE) as a reference electrode. The working electrode (WE) was a carbon steel rod embedded in PVC holder using epoxy resin, so that the circular surface was the working area. Before each measurement, the electrode was immersed in a test solution at open circuit potential (OCP) for 30 min, until a steady state was reached. All polarization curves were recorded by a Voltalab 40 Potentiostat PGZ 301 and a personal computer was used with Voltamaster 4 software at 20 ^{o}C. Each experiment was repeated at least three times to check the reproducibility.

The potentiodynamic polarization measurements were obtained by changing the electrode potential automatically from -800 to -300 mV vs. SCE at open circuit potential with a scan rate 0.2 mV s^{-1} at 20 ^{o}C.

Electrochemical impedance spectroscopy (EIS) measurements were carried out as described elsewhere [22]. A small alternating voltage perturbation (10 mV) was imposed on the cell over the frequency range of 100 kHz to 30 mHz at 20 ^{o}C.

2.6. Surface tension measurements

The surface tension was measured for different concentrations of the synthesized surfactants that dissolved in double distilled water and in 0.5 M H_2SO_4 with a Du Nouy Tensiometer (Kruss Type 6). All solutions were prepared in double distilled water with a surface tension equal to 72 mN m^{-1} at 25 °C.

2.7. Conductivity measurements

An electrical conductivity meter (Type 522; Crison Instrument, S.A.) was used to measure the conductivity of the different surfactant solutions.

3. Results and discussion

3.1. Confirmation of chemical structure

Schiff base ((Z)-2-((pyridin-2-ylimino)methyl)phenol)

FTIR spectra

FTIR spectrum of (Z)-2-((pyridin-2-ylimino)methyl)phenol (Fig. 3) showed that the characteristic bands (cm^{-1}) at 3431.12 (bonded –**OH)**, 3051.41 **(**Ar-**H)** and 1608.52 (**CH=N**).

^{1}HNMR spectra

^{1}HNMR (DMSO - d_6) spectrum showed δ , ppm at: 12.99 (1H, s, O**H**), 9.47 (1H, s, N=C**H**), 8.51, 8.50 (1H, dd, J=3.05, 1.5 Hz, Py-**H**); 7.90, 7.90, 7.89 (1H, ddd, J=7.6, 2.3, 5.35 Hz, Py-**H**), 7.76495, 7.773 (1H, dd, J=1.55, 6.1 Hz, Py-**H**) and three sets multiples at (7.41–7.4425), (7.32–7.34), (6.95–6.97) (5H, Py-**H** + 4 Ar-**H**).

Mass spectrum

The mass spectrum of (Z)-2-((pyridin-2-ylimino)methyl)phenol (Fig. 4) showed that a molecular ion peak m/z 198(17.12%), and other significant peaks are shown at m/z 171 (4.86%) $\mathbf{C_{11}H_9NO}$, 143 (5.63%) $\mathbf{C_{10}H_9N}$, 128 (9.03%) $\mathbf{C_{10}H_8}$.

According to the data of FTIR, ^{1}HNMR and Mass spectroscopy, the product is confirmed as (Z)-2-((pyridin-2-ylimino) methyl) phenol.

Cationic surfactant ((Z)-1-dodecyl-2-(2-hydroxybenzylideneamino)pyridinium bromide)

Elemental analysis

Elemental analysis of (Z)-1-dodecyl-2-(2-hydroxybenzylideneamino)pyridinium bromide as the following: (theoretical, %) C, 64.42; H, 7.88; N, 6.26; O, 3.58; Br, 17.86 and (found, %) C, 64.55; H, 7.79; N, 6.24; O, 3.61; Br, 17.81.

FTIR spectra

FTIR spectrum of (Z)-1-dodecyl-2-(2-hydroxybenzylideneamino)pyridinium bromide showed bonded –**OH** at 3293.31cm^{-1}, **(Ar-H)** aromatic at 3126 cm^{-1}, **(C-H)** aliphatic at 2921.20, 2852.63 cm^{-1} and **CH=N** at 1660.14, 1612.91 cm^{-1}.

^{1}HNMR spectra

^{1}HNMR (DMSO–d_6) spectrum (Fig. 5) showed δ , ppm at: 10.21 ((1H, s, O**H**), 8.5 (1H, s, N=C**H**), three sets of multiples at (7.85–8.07), (7.06–7.07), (6.78–6.95), (4H, Py-**H** + 4H, Ar–**H**), 0.79 (3H, C**H**$_3$), 1.15 (m, 16H, (C**H**$_2$)$_8$), 4.10 (2H, $^{+}$NC**H**$_2$).

According to the data of FTIR, and ^{1}HNMR spectroscopy, the product is (Z)-1-dodecyl-2-(2-hydroxybenzylideneamino) pyridinium bromide.

Schiff base (N,N'-(pentane-1,5-diylidene)dipyridin-2-amine)

FTIR spectra

FTIR spectrum of N,N'-(pentane-1,5-diylidene)dipyridin-2-amine showed **CH** aliphatic at 2953.9, 2923.3, 2843 cm^{-1}, Ar-**H** aromatic at 3078.23, 3015.49 cm^{-1}, **NH** at 3285 cm^{-1} and **CH=N** at 1650.78 cm^{-1}.

^{1}HNMR spectra

^{1}HNMR ($CDCl_3$–d_6) spectrum of N,N'-(pentane-1,5-diylidene)dipyridin-2-amine showed different peaks at δ, ppm : 1.229, 1.942, 2.168 and 2.262 as multi sets for saturated C-**H** protons; 4.87 and 4.941 for olefinic C-**H** protons. Py-**H**, as multi sets at δ: 6.49, 6.63,

6.84, 7.428, 8.057 ppm and N=C**H** at 8.19 and 8.20 ppm. Allylic proton shift indicated by the presence of δ N-**H** at 4.416 ppm as broad absorption.

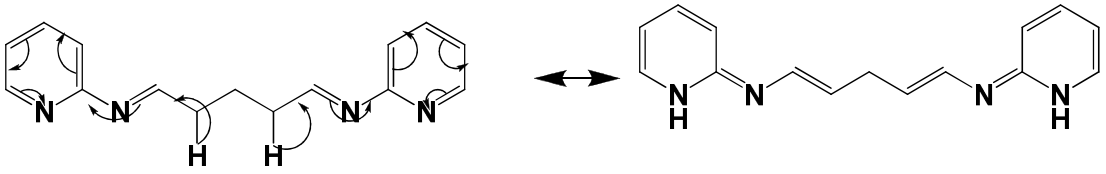

major

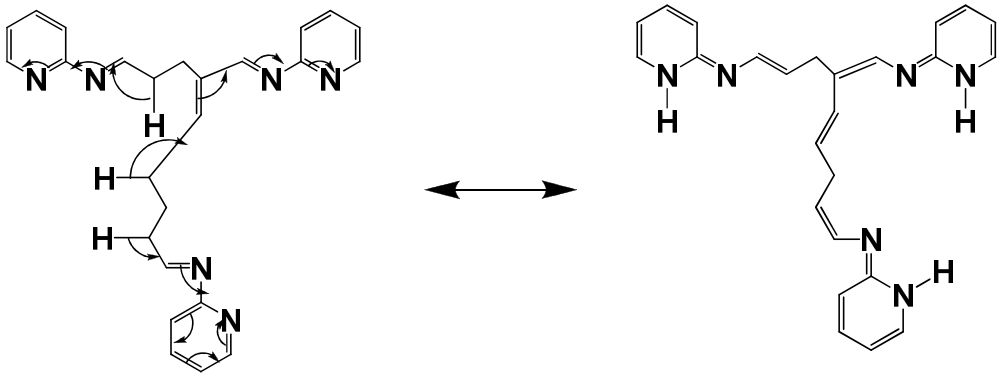

trace

Mass spectra

The mass spectrum of N,N'-(pentane-1,5-diylidene)dipyridin-2-amine (Fig. 6a) showed that a molecular ion peak m/z 252 (0.3%) together with a base peak at 157 while the byproduct (Fig. 6b) gave a molecular ion peak at m/z 410 (28.6 %) together with a base peak at m/z 91.

Fragmentation of major product as follows:

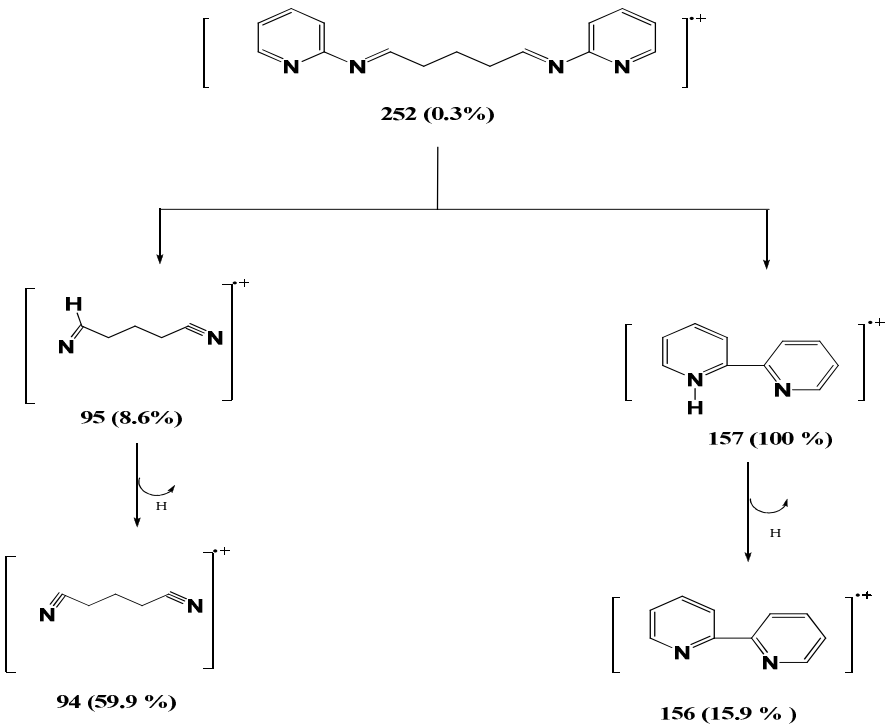

According to the data FTIR, ^{1}HNMR, Mass spectroscopy, the product is a mixture of two compounds: N,N'-(pentane-1,5-diylidene)dipyridin-2-amine (major) and (N,N'E,N,N'E)-N,N'-((E)-2-((E)-5-(pyridin-2-ylimino)pentylidene)pentane-1,5-diylidene)dipyridin-2-amine (trace). The formation of by-product was considered Aldol condensation followed by Schiff base by-product.

Gemini surfactant (2,2'-(pentane-1,5-diylidenebis(azan-1-yl-1-ylidene))bis(1-dodecylpyridinium bromide)

Elemental analysis

Elemental analysis of (Z)-1-dodecyl-2-(2-hydroxybenzylideneamino)pyridinium bromide as the following: (theoretical, %) C, 62.39; H, 8.86; N, 7.46; Br, 21.29 and (found, %) C, 62.71; H, 8.91; N, 7.41; Br, 21.09.

FTIR spectra

FTIR spectrum of 2,2'-(pentane-1,5-diylidenebis(azan-1-yl-1-ylidene))bis(1-dodecylpyridinium bromide) showed two bands at 2926.12 cm^{-1}, 2854.34 cm^{-1} for **C**-H aliphatic and **C=N** stretching appeared band at 1662.41 cm^{-1}.

^{1}HNMR spectra

^{1}HNMR (DMSO–d_6) spectrum of 2,2'-(pentane-1,5-diylidenebis(azan-1-yl-1-ylidene))bis(1-dodecylpyridinium bromide) (Fig. 7) showed different peaks δ, ppm: 0.80 (6H, 2C**H**$_3$); 1.21 (46H, 23C**H**$_2$), 3.46 (4H, 2C**H**$_2$N), 4.08 (2H, 2C**H**-Br), 6.816, 6.927, 7.855, 7.901 (4 sets of multiplets, **2Py-H**) ppm. The presence of δ CH-Br at 4.08 was indicated the presence of non-cationic ((N1E,N5E)-1,5-dibromo-N1,N5-bis(1-dodecylpyridin-2(1H)-ylidene)pentane-1,5-diamine) as trace.

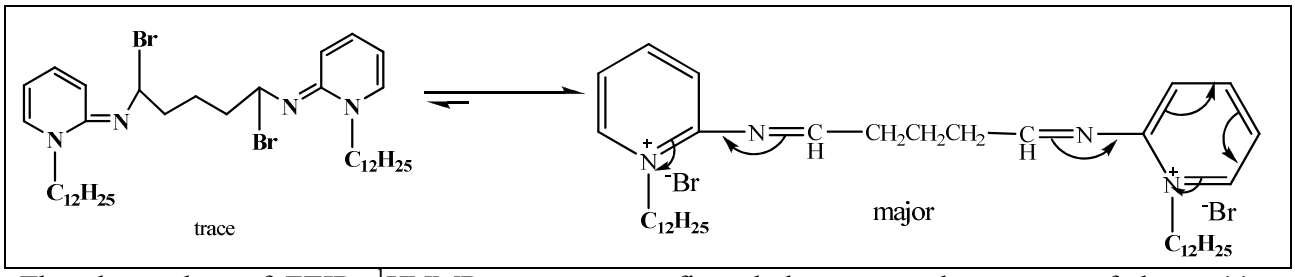

The above data of FTIR, ^{1}HNMR spectrum confirmed the proposed structure of the gemini surfactant (2,2'-(pentane-1,5-diylidenebis(azan-1-yl-1-ylidene))bis(1-dodecylpyridinium bromide).

3.2. Weight loss measurement

The corrosion rate (k) was calculated from the following equation [23]:

$$k = \frac{\Delta W}{St} \qquad (1)$$

where ΔW is the average weight loss of three parallel carbon steel sheets, S is the total area of the specimen and t is immersion time.

Inhibition efficiency (η_w) and surface coverage (θ) were calculated according to the following equations [23]:

$$\eta_W = \left(\frac{W - W_o}{W}\right) \times 100 \qquad (2)$$

$$\theta = \left(\frac{W - W_o}{W}\right) \times 100 \qquad (3)$$

where W and W_o are the weight loss of carbon steel in absence and presence of the inhibitors respectively.

The obtained results showed that the corrosion efficiencies for the cationic and the cationic gemini surfactants increased with increasing the inhibitors concentration.

The values of corrosion rate (k), percentage inhibition efficiency (η_w) and surface coverage (θ) were obtained from weight loss method in the presence and absence of different concentrations of cationic and gemini surfactants at 20-60 ^oC are summarized in Table 1. It was found that, the corrosion rate values were decreased with increasing the inhibitors concentration. The inhibition efficiency of all inhibitors was increased with increasing the concentration. The maximum inhibition efficiency for each compound was obtained at 1×10^{-2} M. From data in Table 1, it was observed that, the synthesized gemini surfactant was showed a good inhibition efficiency by increasing temperature from 20–60 ^oC. This result can related to the chemical adsorption of the inhibitor molecules to the metal surface [24]. On the contrary, the inhibition efficiency of the synthesized cationic surfactant was decreased with increasing the temperature from 20–60 ^oC. This result can be attributed to desorption of the inhibitor molecules to the metal surface at high temperature [25].

3.3. EIS measurement

Nyquist plots for carbon steel in 0.5 M H_2SO_4 in the absence and presence of the synthesized inhibitors at various concentrations are shown in Fig. 8. It was concluded from these plots that the impedance response of carbon steel in 0.5 M H_2SO_4 had significantly altered after the addition of inhibitors into the test solutions. The semicircles were obtained which cut the real axis at higher and lower frequencies. At higher frequency end, the intercept corresponds to solution resistance (R_s) and at lower frequency end; the intercept corresponds to $R_s + R_{ct}$. The difference between these two values gives the charge transfer resistance (R_{ct}).

The Nyquist plots have similar shape for the synthesized inhibitors. The semicircle in all cases was corresponded to a capacitive loop. The semicircle radii depend on the inhibitor concentration. The diameter of the capacitive loop was increased with increasing of inhibitor concentration.

The double layer capacitance (C_{dl}) and (R_{ct}) were calculated from Nyquist plots as described elsewhere [26]. As R_{ct} is inversely proportioned to the corrosion current density, it was used to determine the inhibition efficiency (η_I) from the following equation:

$$\eta_I = \left(\frac{R^o_{ct} - R_{ct}}{R^o_{ct}}\right) \times 100 \qquad (4)$$

where R_{ct} and R^o_{ct} are the charge transfer resistance values in uninhibited and inhibited solutions.

The results obtained from electrochemical impedance spectroscopy (EIS) method can be interpreted in terms of the equivalent circuit of the electrical double layer which has been shown in Fig. 9. Simulation of Nyquist diagrams was made using ZSimpWin program in order to obtain the optimum electrical circuit. The Nyquist plots obtained in the real

system had a general behavior where the double layer on the interface of metal/solution does not behave as a real capacitor. On the metal side electrons control the charge distribution whereas on the solution side it is controlled by ions. Since ions were much larger than the electrons, the equivalent ions to the charge on the metal will occupy quite a large volume on the solution side of the double layer [27]. Therefore CPE used in place of double layer capacitance, C_{dl}, to represent the non-ideal capacitive behavior of the double layer. Its impedance is described by the expression [28]:

$$Z_{CPE} = \frac{1}{Y_o(j\omega)^n} \quad (5)$$

where Y_o is a proportional factor, $J^2 = -1$, $\omega = 2\pi f$ and n is the phase shift. For $n = 0$, Z_{CPE} represents a resistance with $R = Y^{-1}$, for $n = 1$ a capacitance with $C = Y$, for $n = 0.5$ a Warburg impedance with $W = Y$ and for $n = -1$ an inductive with $L = Y^{-1}$. The double layer capacitances, C_{dl}, for a circuit including a *CPE* were calculated from the following equation [28]:

$$C_{dl} = Y_o(\omega_{max})^{n-1} \quad (6)$$

where Y_o is a proportional factor and $\omega_{max} = 2\pi f_{max}$ and f_{max} is the frequency at which the imaginary component of the impedance is maximal.

The electrochemical impedance parameters derived from the Nyquist plots and the inhibition efficiency (η_I) are shown in Table 2. It is clear that R_s values were changed in the presence of inhibitor in its absence. The increase in the synthesized surfactants concentration can cause a change in a small percent of the overall solution conductivity. From the Table 2, it is clear that charge transfer resistance values increased and the capacitance values decreased with increasing inhibitors concentration. The decreasing in the capacitance, which can resulted from a decrease in local dielectric constant and/or an

increase in the thickness of the electrical double layer, was suggested that the inhibitor molecules acted by adsorption at the metal/solution interface [29]. This indicated the formation of a surface film on the carbon steel. The addition of synthesized inhibitors provided lower C_{dl} values, probably as a consequence of replacement of water molecules by inhibitors bases at the electrode surface. Also the inhibitor molecules may reduce the capacitance by increasing the double layer thickness according to the Helmholtz model [28].

$$\delta_{org} = \frac{\varepsilon \varepsilon_o A}{C_{dl}} \qquad (7)$$

where ε is the dielectric constant of the medium, ε_o is the vacuum permittivity, A is the electrode surface area and δ_{org} is the thickness of the protective layer.

The value of C_{dl} was always smaller in the presence of the inhibitor than in its absence, which due to result from the effective adsorption of the synthesized inhibitors [30].

As seen from Fig. 10, Bode plots refer to the existence of an equivalent circuit that contains a single constant phase element in the metal/solution interface. The increase of absolute impedance at low frequencies in Bode plot confirmed the higher protection with increasing the concentration of the inhibitor, which is related to adsorption of the inhibitor on the carbon steel surface [31]. Fig. 10 was showed that the phase angle depression at relaxation frequency decreased with increasing the inhibitor concentration which indicated the capacitive response increased with increasing the inhibitor concentration. This behavior can attributed to the corrosion activity that was decreased with increasing the concentration of both cationic and gemini surfactants. The standard deviation average of three replicates was 0.34.

3.4. Potentiodynamic polarization measurements

The anodic and the cathodic polarization curves, for carbon steel in 0.5 M H_2SO_4 in the absence and presence of different concentrations of inhibitors, are shown in Fig. 11. It was observed from Fig. 11 that both of cathodic and anodic curves showed a lower current density in the presence of the prepared surfactants than those recorded in the 0.5 M H_2SO_4 solution alone. This behavior indicates that these surfactants had significant effects on both of cathodic and anodic reactions of corrosion process which suggest that these inhibitors acts as mixed type inhibitors [32]. This behavior is due to the synthesized cationic and gemini surfactants adsorbed to the metal surface via the quaternary nitrogen atom (N^+), counter ion (Br^-) and π-electrons of aromatic ring and lone pair of electrons of nitrogen atoms of azomethine group (-CH=N-). Quaternary nitrogen atom (N^+) is adsorbed on the cathodic sites to decrease the evolution of hydrogen while the counter ion (Br^-) and π-electrons of aromatic ring and lone pair of electrons of nitrogen atoms of azomethine group (-CH=N-) are adsorbed on the anodic sites to reduce the anodic dissolution.

The inhibition efficiency, (η_p), was calculated from the following equation [33]:

$$\eta_p = \left(\frac{i_{corr} - i^{o}_{corr}}{i_{corr}}\right) \times 100 \qquad (8)$$

where i_{corr} and i^{o}_{corr} are the corrosion current density values without and with inhibitor, respectively.

The electrochemical parameters such as corrosion potential (E_{corr}), corrosion current density (i_{corr}), cathodic and anodic Tafel slopes (β_c and β_a) and inhibition efficiency (η_p) values were obtained from polarization curves are given in Table 3. It was clearly reported in Table 3 that, the inhibition efficiency was increased and the corrosion current densities was decreased by increasing the inhibitors concentration. Moreover, Table 3

results were showed that the corrosion potentials of inhibitors were slightly shifted in the positive direction. The electrochemical processes on the metal surface were likely to be closely related to the adsorption of the inhibitors, and the adsorption depends on the chemical structure of the inhibitors [34]. The values of cathodic Tafel slope (β_c) and anodic Tafel slope (β_a) for the synthesized inhibitors were slightly shifted in the presence of inhibitor. The slight variations in Tafel slope was suggested that the synthesized inhibitors affects the kinetics of the hydrogen evolution reaction without change the mechanism of iron dissolution [35]. The average of the standard deviation for the three replicates was 0.37.

3.5. Adsorption isotherm and thermodynamic parameters

The mechanism of corrosion inhibition may be explained on basis of adsorption behavior. The adsorption of organic inhibitor molecules from the aqueous solution can be regarded as a quasi-substitution process between the organic compound in the aqueous phase [$Org_{(sol)}$] and water molecules at the electrode surface [$H_2O_{(ads)}$]

$$Org_{(sol)} + \times H_2O_{(ads)} \leftrightarrow Org_{(ads)} + \times H_2O_{(sol)} \qquad (9)$$

where × is the size ratio, that is, the number of water molecules replaced by one organic inhibitor.

In this situation, the adsorption of the synthesized surfactants was accompanied by desorption of water molecules from the surface. The degree of surface coverage (θ) for different inhibitor concentrations of all inhibitors were evaluated from the weight loss data. Several adsorption isotherms were tested to describe the adsorption behavior of all compounds used in this study. The Langmuir isotherm is given by following equation:

$$\frac{C}{\theta} = \frac{1}{K_{\text{ads}}} + C \qquad (10)$$

where C is the concentration of inhibitor, K_{ads} is the equilibrium constant of the adsorption process, and θ is the surface coverage.

The Langmuir adsorption plots (Fig. 12) of the synthesized inhibitors gave straight lines with slope equal 1 which indicated that the studied compounds obeyed Langmuir adsorption isotherm. The adsorption equilibrium constant (K_{ads}) equal reciprocal intercept in Fig. 13 for both cationic and gemini surfactants at different concentrations and temperatures was calculated and listed in Table 4. It was found that the high values of both cationic and gemini surfactants reflected the high adsorption ability of these inhibitors on carbon steel surface in 0.5 M H_2SO_4. But the adsorption of the gemini surfactant was more efficient than the cationic surfactant. This is due to the gemini surfactant has more adsorption centers than the cationic surfactant.

The standard free energy of adsorption (ΔG^{o}_{ads}) was calculated using the following equation [36] and listed in Table 4.

$$\Delta G^{o}_{ads} = -RT \ln(55.5 K_{ads}) \qquad (10)$$

where ΔG_{ads} is the free energy of adsorption, K_{ads} is the equilibrium constant for adsorption desorption process, R is the gas constant, T is the absolute temperature and 55.5 is the molar concentration of water.

The negative value of ΔG^{o}_{ads} suggested that the adsorption of the inhibitors, in 0.5 M H_2SO_4 on the carbon steel surface, was more stable. Generally, ΔG^{o}_{ads} values around -20 kJ mol^{-1} or lower were consistent with the electrostatic interaction between the charged molecules and the charged metal (physisorption) while those around -40 kJ mol^{-1} or higher were involved sharing or transferring of electrons from organic molecules to the metal surface to form a coordinate bond (chemisorption) [1,37,38]. The calculated ΔG^{o}_{ads}

values at various temperatures were found to be from -31.84 to -35.92 kJ mol^{-1} for cationic surfactant and from -31.94 to -38.43 kJ mol^{-1} for gemini surfactant at various temperatures. ΔG^{o}_{ads} values indicated that the adsorption process involved both the physical and chemical adsorption [39].

The standard enthalpy of adsorption, ΔH^{o}_{ads}, was calculated according to the Van't Hoff equation [40,41]:

$$\ln K_{ads} = \left(\frac{-\Delta H^{o}_{ads}}{RT}\right) + \text{constant} \qquad (11)$$

To obtain the standard enthalpy of adsorption, the relationship between ln K_{ads} and $1/T$ is shown in Fig. 13. The negative sign of ΔH^{o}_{ads} values for cationic surfactant indicated that the adsorption of inhibitor molecules was an exothermic process [20] while the positive sign of ΔH^{o}_{ads} values for gemini surfactant indicated that the adsorption of inhibitor molecules was an endothermic process [19].

According to the thermodynamic basic equation, the standard adsorption entropy, ΔS^{o}_{ads}, was calculated from the following equation [42]:

$$\Delta G^{o}_{ads} = \Delta H^{o}_{ads} - T\Delta S^{o}_{ads} \qquad (12)$$

All the obtained thermodynamic parameters were given in Table 4. It was found that the adsorption of inhibitor molecules is accompanied by positive values of ΔS^{o}_{ads} which may be explained by an ordered layer onto the steel surface.

3.6. Mechanism of inhibition

Corrosion inhibition of carbon steel in acidic solutions by different inhibitors can be explained on the basis of molecular adsorption. The compounds were inhibited corrosion by controlling both anodic as well as cathodic reactions. The different types of adsorption may be considered for the adsorption of cationic and gemini surfactants molecules at the

metal surface: (i) electrostatic attraction between the charged molecules and the charged metal, (ii) interaction of unshared electron pairs in the molecule with the metal, and (iii) a combination of the above [43,44].

The synthesized cationic and gemini surfactants adsorbed to the metal surface via the quaternary nitrogen atom (N^+) and counter ion (Br^-). Quaternary nitrogen atom (N^+) adsorbed on the cathodic sites to decrease the evolution of hydrogen while the counter ion (Br^-) adsorbed on the anodic sites to reduce the anodic dissolution. The adsorption on anodic site occurred through π-electrons of aromatic ring and lone pair of electrons of nitrogen atoms of azomethine group (-CH=N-) in both cationic and gemini surfactant which decreased the anodic dissolution of carbon steel. The high performance of two inhibitors was attributed to the presence of many adsorption centers, larger molecular size and the planarity of compounds. The inhibition efficiency of the gemini surfactant were higher than those of the cationic surfactant at different concentrations and temperatures. The gemini surfactant has been found to give the better performance. This may be attributed to the higher dipole moment than cationic surfactant and due to the presence of two azomethine groups, two quaternary nitrogen atoms and two Br^- ions in this compound while cationic surfactant has one azomethine group, one quaternary nitrogen atom and one Br^- ion.

The adsorption of studied cationic and gemini inhibitors on carbon steel surface obeyed Langmuir adsorption isotherm because the inhibitors form monolayer in the concentrations range used in this study as shown in the relation between inhibition efficiency and concentration (where there one S curve only). The adsorption of gemini surfactants on metal surface is more complicated than that of conventional surfactants

because the gemini surfactants contain two hydrophilic groups and two hydrophobic groups.

The adsorption of gemini surfactant on the steel surface in acidic medium reflects three different modes of adsorption:

(1) At low concentrations, it seems that the adsorption takes place by horizontal binding to hydrophobic region (Fig. 14a). This adsorption is favored by an electrostatic interaction between the two ammonium groups (N^+) and cathodic sites on one hand and Br^- ion on the metallic surface on the other hand.

(2) When the inhibitor concentration increases, a perpendicular adsorption takes place as a result of an inter-hydrophobic chain interaction (Fig. 14b).

(3) At higher inhibition concentrations, a perpendicular adsorption of surfactant continues with the hydrophilic group protruding into the solution and the hydrocarbon tail mingling with the adsorbed monomers, driven by the hydrophobic force, until the surface is saturated (Fig. 14c).

3.7. The comparison between the synthesized surfactants and some Schiff bases, synthesized as precursors

The anticorrosive effect of the Schiff bases, synthesized as precursors ((Z)-2-((pyridin-2-ylimino)methyl)phenol and N,N'-(pentane-1,5-diylidene)dipyridin-2-amine), on the corrosion of carbon steel in 0.5 M H_2SO_4 was examined, in comparison with the anticorrosive effect of the synthesized surfactants by weight loss measurements at the same conditions. It was found that at 1×10^{-2} M and 20 ^oC, the inhibition efficiency of the synthesized cationic surfactant (94.0 %) is higher than Schiff bases (((Z)-2-((pyridin-2-ylimino)methyl)phenol) (88.7 %). Also, at 1×10^{-2} M and 20 ^oC, the inhibition

efficiency of the synthesized gemini surfactant (96.7 %) is higher than Schiff bases (N,N'-(pentane-1,5-diylidene)dipyridin-2-amine)), synthesized as precursors, (90.2 %). This is due to the synthesized compound regard as cationic and gemini surfactants, however, Schiff bases reported in the literature are ordinary organic compounds. Surfactants that lower the surface tension (or interfacial tension) between corrosive medium and steel surface and also act as dispersants. Therefore, surfactants up to critical micelle concentration (C_{cmc}) will diffuse out of the bulk water phase and are adsorbed at the interfaces between carbon steel and corrosive medium. On the other side, organic compounds will diffuse both in bulk solution and interface by the same rate nearly. In addition, surfactant up to C_{cmc} form thin film on steel surface involved two inhibitive factors; one hydrophilic group involved hetero atoms and other water-insoluble hydrophobic group. But Schiff bases adsorbed on steel surface through only one inhibitive factor, hetero atoms.

3.7. Surface active properties

3.7.1. The surface tension

The surface tension values (γ) of the surfactants were measured for a range of concentrations above and below the critical micelle concentration (C_{cmc}). A representative plot of γ versus -log concentration of cationic and gemini surfactants in both bidistilled water and 0.5 M H_2SO_4 is shown in Figs. 15 and 16. A linear decrease in surface tension was observed with the increasing the surfactant concentration. This observation was recorded for the synthesized surfactants up to the C_{cmc}, beyond which no considerable changes were noticed. This common behavior is shown by surfactants in solution and was used to determine their purity and C_{cmc}'s. The C_{cmc} values obtained from the break point in the γ–log C plots are listed in Table 5. The γ–log C plots also provided

information about area per molecule at air-water interface, effectiveness and surface excess concentration of surfactant ions of the synthesized surfactants. C_{cmc} and other surface properties of all synthesized surfactants were determined also in 0.5 M H_2SO_4 and are listed in Table 5.

Comprising C_{cmc} for both cationic and gemini surfactants demonstrated that increasing the number of the hydrocarbon chain had the tendency of lowering the concentration at which aggregation was initiated. Therefore C_{cmc} of gemini surfactant is smaller than cationic surfactant due to the hydrocarbon chain length.

3.7.2. Effectiveness (π_{cmc})

The maximum surface pressure (π_{cmc}) which is defined as the effectiveness of a surfactant in reducing surface tension was calculated from the following equation [45]:

$$\pi_{cmc} = \gamma_o - \gamma_{cmc} \qquad (13)$$

where γ_o and γ_{cmc} are the surface tensions of pure water and surface tension at C_{cmc}, respectively. π_{cmc} values are listed in Table 5. It was found that, effectiveness of gemini surfactant is higher than cationic surfactant due to the increasing the number of alkyl chain. Also, C_{cmc} and surface pressure (π_{cmc}) values decreased in 0.5 M H_2SO_4 than in water. These phenomena are related to the famous Hofmeister series [46-48], which is an empirical measure of ions' hydration degree. The Hofmeister series orders ions with increased salting-in potency from left to right as follows:

$SO_4^{-2} > HPO_4^{-2} > OH^- > F^- > HCOO^- > CH_3COO^- > Cl^- > Br^- > NO_3^- > I^- > SCN^- > ClO_4^-$

The basis for this ordering was related to an individual anion's ability to penetrate the head group region of the monolayer, thereby disrupting the hydrocarbon packing [49, 50]. The species to the left of Cl^- were referred to as kosmotropes, while those to its right

are called chaotropes. These terms originally referred to an ion's ability to alter the hydrogen bonding network of water [51]. The kosmotropes, which were believed to be 'water structure makers', were strongly hydrated and have stabilizing and salting-out effects on surfactant. On the other hand, chaotropes ('water structure breakers') are known to destabilize folded hydrophobic part and give rise to salting-in behavior. Kosmotropic anions as SO_4^{-2}, producing high electric fields at short distances, bind their water molecules strongly and compete efficiently for water with the hydrophilic part of both the synthesized cationic and cationic gemini surfactants. This phenomenon leads to the dehydration of the surfactant molecule's hydrophilic part, an effect which depresses the C_{cmc} value of the synthesized cationic and cationic gemini surfactants and increases attractive interactions between these micelles.

3.7.3. The surface excess (Γ_{max})

The surface excess concentration of surfactant ions, Γ_{max}, was provided an effective measure of the surfactant adsorption at the air/water interface. The maximum value of the surface excess concentration was in corresponds with the maximum concentration that a surfactant can attain at the interface, Γ_{max}, and it was defined as the effectiveness of adsorption at an interface. The concentration of the surfactant was always higher at the surface phase than that in the bulk solution. The Γ_{max} values were calculated from the slope of the straight line in the surface tension plot ($d\gamma/d \ln C$) below C_{cmc}, using the appropriate form of Gibbs adsorption equation [52]:

$$\Gamma_{\max} = \left(\frac{-1}{nRT}\right)\left(\frac{d\gamma}{d \ln C}\right) \qquad (14)$$

where Γ_{max} is the surface excess concentration of surfactant ions, R is gas constant, T is absolute temperature, C is concentration of surfactant, γ is surface tension at given concentration and n is number of species ions in solution.

The values of the surface excess concentration were calculated and listed in Table 5. It was found that, surface excess concentration increased by increasing the number of carbon chain length, which could be due to the hydrophobic effect of carbon chain.

3.7.4. The area per molecule (A_{min})

The minimum surface area per adsorbed molecule, A_{min} (nm^2), is defined as the area occupied by each molecule at the liquid/air interface. A_{min} was calculated from the following equation [53,54]:

$$A_{min} = \frac{10^{14}}{N_A \Gamma_{max}} \qquad (15)$$

where N_A is the Avogadro's number and Γ_{max} is the maximal surface excess of adsorbed surfactant molecules at the interface.

The values of area per molecule were calculated and listed in Table 5. It was found that A_{min} values of the gemini surfactant were smaller than that of the cationic surfactant. That can be attributed to the increasing numbers of head groups and alkyl chains. A_{min} value of both cationic and gemini surfactants in 0.5 M H_2SO_4 were smaller than in water due to the increase in dehydration of the surfactant molecule's hydrophilic part.

3.8. Conductivity measurements

Specific conductivity (K) measurements were performed for the prepared cationic and gemini surfactants at 20 ^oC in order to evaluate the C_{cmc} and the degree of counter ion dissociation, β. It is well known that, the specific conductivity was linearly correlated to the surfactant concentration in both the premicellar and in the postmicellar regions, and

the slope in the premicellar region greater than that in the postmicellar region [55]. The intersection point between the two straight lines gave the C_{cmc} while the ratio between the slopes of the postmicellar region to that in the premicellar region gives counter ion dissociation, β.

Fig. 17 showed the relation between specific conductivity and concentration of the synthesized surfactants. The degree of counter ion dissociation values were calculated and listed in Table 5. It was found that, the degree of dissociation of the gemini surfactant was higher than that of the cationic surfactant, due to the increase in the cation bulkiness. The C_{cmc} values, which determined using electrical conductivity, were in agreement with those obtained using surface tension.

3.9. The standard free energy of micelle formation (ΔG^{o}_{mic})

The C_{cmc} of a surfactant was regarded as a measure of the stability of its micellar form relative to its monomeric form. In the charged pseudophase model of micelle formation, the standard free energy of micelle formation per mole of surfactant was calculated by the following equation [22]:

$$\Delta G^{o}_{mic} = (2 - \beta) RT \ln C_{cmc} \qquad (16)$$

where R is the gas constant, T is the temperature, β is the degree of counter ion dissociation and C_{cmc} is expressed in the molarity of the surfactant.

ΔG^{o}_{mic} values were calculated and listed in Table 5. It is clear that, ΔG^{o}_{mic} values of the gemini surfactant were lower than the cationic surfactant. This result means that the micelle formation was thermodynamically favored for the gemini surfactant than the cationic surfactant.

3.10. The relation between corrosion inhibition and surface properties of the prepared surfactants

Generally, surfactant is amphiphilic compound that contains hydrophobic group (tail) and hydrophilic groups (head) [56]. Ordinary cationic surfactant contains one hydrophobic group and one hydrophilic group while gemini surfactant contains two hydrophobic group and two hydrophilic group connected by spacer. Gemini surfactants are more efficient at low surface tension and have much lower critical micelle concentration values (C_{cmc}) than conventional surfactants. Surfactants, up to critical micelle concentration (C_{cmc}), will diffuse out of the bulk water-phase and adsorb at the interfaces between carbon steel and corrosive medium. Therefore, migration of gemini surfactant is faster than cationic surfactant. Thus, concentration of gemini surfactant at interface, between steel surface and corrosive solution, is higher than cationic surfactant at the same concentration [52,56]. This is due to surface tension and C_{cmc} of gemini surfactant that are smaller than cationic surfactant. The highest reduction in the surface tension (effectiveness, π_{cmc}) was achieved by the gemini surfactant compared to that obtained by the cationic surfactant. This is in a good agreement with the inhibition efficiency results which achieved by the gemini surfactant. It seems that the synthesized surfactants were favored adsorption rather than micellization. The fact that ΔG^{o}_{ads} was more negative compared to the corresponding ΔG^{o}_{mic} could be taken as a strong evidence on the feasibility of the adsorption of the synthesized surfactants. It was noticed that, the Γ_{max} value of the gemini surfactant was higher than the cationic surfactant. On the other hand, the A_{min} value of the gemini surfactant was lower than the cationic surfactant considering this one explain why gemini surfactant was more effective than cationic

surfactant. All these parameters explain why gemini surfactant was effective inhibitor than cationic surfactant.

4. Conclusions

1. Novel cationic and gemini surfactants were successfully synthesized, purified and characterized.
2. The corrosion inhibition efficiency of the gemini surfactant was higher than the cationic surfactant at the same concentration and temperature. The maximum inhibition efficiency was at 1×10^{-2} M.
3. Inhibition efficiency increases with increase in the concentration of both the synthesized cationic and gemini surfactants and decreases with increasing the temperature.
4. Inhibition efficiency increases with increase in the temperature for the synthesized cationic surfactant and decreases with increase in the temperature for the synthesized gemini surfactant.
5. The adsorption of the prepared inhibitors, on the carbon steel, obeyed the Langmuir adsorption isotherm model. The adsorption process involved both the physical as well as chemical adsorption but physical adsorption more efficient than chemisorption for cationic surfactant and chemisorption more efficient than physical adsorption for gemini surfactant
6. The synthesized cationic and gemini surfactants had good surface properties but the gemini surfactant was better than the cationic surfactant. C_{cmc} and surface pressure values were decreased in 0.5 M H_2SO_4 than in water.

7. The prepared inhibitors acted as mixed-type inhibitor for carbon steel in 0.5 M H_2SO_4.
8. The value of C_{dl} was always smaller in the presence of the inhibitor than in its absence, which due to result from the effective adsorption of the synthesized inhibitors.
9. The inhibition efficiency calculated from potentiodynamic polarization, electrochemical impedance spectroscopy and electrochemical frequency modulation measurements are in good agreement.

References

[1] M.A. Hegazy and A.S. El-Tabei, Synthesis, surface properties, synergism parameter and inhibitive performance of novel cationic gemini surfactant on carbon steel corrosion in 1 M HCl solution, J. Surfact. Deterg. 16 (2013) 221–232.

[2] P.C. Okafor, Y. Zheng, Synergistic inhibition behaviour of methylbenzyl quaternary imidazoline derivative and iodide ions on mild steel in H_2SO_4solutions, Corros. Sci. 51 (2009) 850-859.

[3] H.L. Wang, R.B. Liu, J. Xin, Inhibiting effects of some mercapto-triazole derivatives on the corrosion of mild steel in 1.0 M HCl medium, Corros. Sci. 46 (2004) 2455-2466.

[4] O. Benali, L. Larabi, B. Tabti, Y. Harek, Influence of 1-methyl 2-mercapto imidazole on corrosion inhibition of carbon steel in 0.5 M H_2SO_4, Anti-Corros. Method Mater. 52 (2005) 280-285.

[5] A.S. Fouda, A.A. Al-Sarawy, E.E. El-Katori, Pyrazolone derivatives as corrosion inhibitors for C-steel in hydrochloric acid solution, Desalination 201 (2006) 1-13.

[6] B. Ramesh Babu, K. Thangavel, The effect of isomers of some organic compounds as inhibitors for the corrosion of carbon steel in sulfuric acid,Anti-Corros. Method Mater. 52 (2005) 219-225.

[7] A.S. Fouda, H.A. Mostafa, F. El-Taib Haekel, G.Y. Elewady, Synergistic influence of iodide ions on the inhibition of corrosion of C-steel in sulphuric acid by some aliphatic amines, Corros. Sci. 47 (2005) 1988-2004.

[8] M.A. Hegazy, Novel cationic surfactant based on triazole as a corrosion inhibitor for carbon steel in phosphoric acid produced by dihydrate wet process, J. Mol. Liq. 208 (2015) 227-236.

[9] M. Lebrini, M. Lagrenee, H. Vezin, L. Gengembre, F. Bentiss, Electrochemical and quantum chemical studies of new thiadiazole derivatives adsorption on mild steel in normal hydrochloric acid medium, Corros. Sci. 47 (2005) 485-494.

[10] F. Bentiss, M. Lebrini, M. Lagrenee, Thermodynamic characterization of metal dissolution and inhibitor adsorption processes in mild steel/2,5-bis(*n*-thienyl)-1,3,4-thiadiazoles/hydrochloric acid system, Corros. Sci. 47 (2005) 2915-2931.

[11] F. Bentiss, M. Traisnel, H. Vezin, H.F. Hildebrand, M. Lagrenee, 2,5-Bis(4-dimethylaminophenyl)-1,3,4-oxadiazole and 2,5-bis(4-dimethylaminophenyl)-1,3,4-thiadiazole as corrosion inhibitors for mild steel in acidic media, Corros. Sci. 46 (2004) 27812-792.

[12] M. Lebrini, F. Bentiss, H. Vezin, M. Lagrenée, The inhibition of mild steel corrosion in acidic solutions by 2,5-bis(4-pyridyl)-1,3,4-thiadiazole: Structure–activity correlation, Corros. Sci. 48 (2006) 1279-1291.

[13] M. Lebrini, M. Lagrenee, H. Vezin, M. Traisnel, F. Bentiss, Experimental and theoretical study for corrosion inhibition of mild steel in normal hydrochloric acid solution by some new macrocyclic polyether compounds, Corros. Sci. 49 (2007) 2254-2269.

[14] M.A. Migahed, M.A. Hegazy M A, M.A. Al-Sabagh, Synergistic inhibition effect between Cu^{2+} and cationic gemini surfactant on the corrosion of downhole tubing steel during secondary, Corros. Sci. 61 (2012) 10-18.

[15] Z. Jing-Mao, L. Jun, Corrosion Inhibition Performance of Carbon Steel in Brine Solution Containing H_2S and CO_2 by Novel Gemini Surfactants, Acta Phys. -Chim. Sin. 28 (2012) 623-629.

[16] Q. Zhang, Z. Gao, F. Xu, X. Zou, Adsorption and corrosion inhibitive properties of gemini surfactants in the series of hexanediyl-1,6-bis-(diethyl alkyl ammonium bromide) on aluminium in hydrochloric acid solution, Colloids and Surfaces A: Physicochemical and Engineering Aspects. 380 (2011) 191-200.

[17] Y.K. Agrawal, J.D. Talati, M.D. Shah, M.N. Desai, N.K. Shah, Schiff bases of ethylenediamine as corrosion inhibitors of zinc in sulphuric acid, Corros. Sci. 46 (2004) 633-651.

[18] K.C. Emregul, R. Kurtaran, O. Atakol, An investigation of chloride-substituted Schiff bases as corrosion inhibitors for steel, Corros. Sci. 45 (2003) 2803-2817.

[19] A.S. El-Tabei, M.A. Hegazy, A.H. Bedair, M.A. Sadeq, Synthesis and inhibition effect of a novel Tri-cationic surfactant on carbon steel corrosion in 0.5 M H_2SO_4 solution, J. Surfact. Deterg. 17 (2014) 341-352.

[20] M.A. Hegazy, S.S. Abd El Rehim, A.M. Badawi, M.Y. Ahmed, Studying the corrosion inhibition of carbon steel in hydrochloric acid solution by 1-dodecyl-methyl-1H-benzo[d][1,2,3]triazole-1-ium bromide, RSC Adv. 5 (2015) 49070 - 49079.

[21] A.S. El-Tabei, M.A. Hegazy, Synthesis and Characterization of a Novel Nonionic Gemini Surfactant as Corrosion Inhibitor for Carbon Steel in acidic solution, Chem. Eng. Commun. 7 (2015) 851-863.

[22] A.I. Khalaf and M.A. Hegazy, Synthesis and characterization of cationic surfactants for preparation of organobentonite and study their effeteness on the properties of styrene butadiene rubber/bentonite composites, High Performance Polymers 25 (2013) 115–125.

[23] M. Behpour, S.M. Ghoreishi, N. Soltani, M. Salavati-Niasari, M. Hamadanian, A. Gandomi, Electrochemical and theoritical investigation on the corrosion inhibition of mild steel by thiosalicylaldehyde derivatives in hydrochic acid solution, Corros. Sci. 50 (2008) 2172-2181.

[24] Mohamed H.M. Hussein, Mohamed F. El-Hady, Hassan A.H. Shehata, M.A. Hegazy, Hassan H.H. Hefni, Preparation of Some Eco-friendly Corrosion Inhibitors Having Antibacterial Activity from Sea Food Waste, J. Surfact. Deterg. 16 (2013) 233–242.

[25] S.K. Shukla, M.A. Quraishi, 4-Substituted anilinomethylpropionate: New and efficient corrosion inhibitors for mild steel in hydrochloric acid solution, Corros. Sci. 51 (2009) 1990–1997.

[26] A.S. El-Tabei, M.A. Hegazy, Application of the synthesized novel 3,6,9,12,15,18,21-heptaoxatricosane-1,23-diyl bis(4-((4-(dimethylamino)benzylidene)amino)benzoate) as a corrosion inhibitor for carbon steel in acidic media, J. Disp. Sci. and Tech. 35 (9) (2014) 1289-1299.

[27] M Özcan, İ Dehri, M Erbil, Organic sulphur-containing compounds as corrosion inhibitors for mild steel in acidic media: correlation between inhibition efficiency and chemical structure, Appl. Surf. Sci. 236 (2004) 155–164.

[28] M.A. Hegazy, Ahmed Abdel Nazeer, K. Shalabi, Electrochemical studies on the inhibition behavior of copper corrosion in pickling acid using quaternary ammonium salts, J. Mol. Liq. 209 (2015) 419-427.

[29] R.A. Prabhu, T.V. Venkatesha, A.V. Shanbhag, G.M. Kulkarni, R.G. Kalkhambkar, Inhibition effects of some Schiff's bases on the corrosion of mild steel in hydrochloric acid solution, Corros. Sci. 50 (2008) 3356–3362.

[30] M.A. Hegazy, A.S. El-Tabei, H.M. Ahmed, Synthesis of nonionic surfactants and their inhibitive action on carbon steel in hydrochloric acid, Corros. Sci. 64 (2012) 115–125.

[31] M. Mahdavian, S. Ashhari, Corrosion inhibition performance of 2-mercaptobenzimidazole and 2-mercaptobenzoxazole compounds for protection of mild steel in hydrochloric acid solution, Electrochim. Acta 55 (2010) 1720–1724.

[32] A.S. El-Tabei and M.A. Hegazy, A corrosion inhibition study of a novel synthesized gemini nonionic surfactant for carbon steel in 1 M HCl solution, J. Surfact. Deterg. 16 (2013) 757–766.

[33] A. Bouyanzer, B. Hammouti, L. Majidi, Pennyroyal oil from Mentha pulegium as corrosion inhibitor for steel in 1 M HCl, Mater. Lett. 60 (2006) 2840-2843.

[34] Hui-Long Wang, Hong-Bo Fan, Jia-Shen Zheng, Corrosion inhibition of mild steel in hydrochloric acid solution by a mercapto-triazole compound, Mater. Chem. Phys. 77 (2002) 655-661.

[35] N.A. Negm, Y.M. Elkholy, M.K. Zahran, S.M. Tawfik, Corrosion inhibition efficiency and surface activity of benzothiazol-3-ium cationic Schiff base derivatives in hydrochloric acid, Corrosion Science 52 (2010) 3523–3536

[36] G. Quartarone, M. Battilana, L. Bonaldo, T. Tortato, Investigation of the inhibition effect of indole-3-carboxylic acid on the copper corrosion in 0.5 M H_2SO_4, Corros. Sci. 50 (2008) 3467–3474.

[37] Mohammed A. Amin, M.A. Ahmed, H.A. Arida, Taner Arslan, Murat Saracoglu, Fatma Kandemirli, Corros. Sci. 53 (2010) 540-548.

[38] R. Solmaz, Investigation of the inhibition effect of 5-((E)-4-phenylbuta-1,3-dienylideneamino)-1,3,4-thiadiazole-2-thiol Schiff base on mild steel corrosion in hydrochloric acid, Corros. Sci. 52 (2010) 3321–3330

[39] X. Li, S. Deng, H. Fu, Benzyltrimethylammonium iodide as a corrosion inhibitor for steel in phosphoric acid produced by dihydrate wet method process, Corros. Sci. 53 (2011) 664–670

[40] X. Wang, H. Yang, F. Wang, A cationic gemini-surfactant as effective inhibitor for mild steel in HCl solutions, Corros. Sci. 52 (2010) 1268–1276.

[41] M.R. Noor El-Din, A.M. Al-Sabagh, M.A. Hegazy, Study of the inhibition efficiency for some novel surfactants on the carbon steel (Type H-11) pipelines in

0.5 M HCl solution by potentiodynamic technique, J. Disp. Sci. and Tech. 33 (2012) 1444–1451.

[42] Z. Tao, S. Zhang, W. Li, B. Hou, Corrosion inhibition of mild steel in acidic solution by some oxo-triazole derivatives, Corros. Sci. 51 (2009) 2588–2595.

[43] M. Benabdellah, A. Aouniti, A. Dafali, B. Hammouti, M. Benkaddour, A. Yahyi, A. Ettouhami, Investigation of the inhibitive effect of triphenyltin 2-thiophene carboxylate on corrosion of steel in 2 M H_3PO_4 solutions, Appl. Surf. Sci. 252 (2006) 8341-8347.

[44] R. Solmaz, G. Kardas, B. Yazıcı, M. Erbil, Adsorption and corrosion inhibitive properties of 2-amino-5-mercapto-1,3,4-thiadiazole on mild steel in hydrochloric acid media, Colloids Surf. A: Physicochem. Eng. Aspects 312 (2008) 7-17.

[45] P. Kutej, J. Vosta, J. Pancir, N. Hackerman, Electrochemical and quantum chemical study of propargyl alcohol adsorption on iron, J. Electrochem. Soc. 142 (1995) 1847-1850.

[46] F. Hofmeister, Zur Lehre von der Wirkung der Salze, [Title translation: About the science of the effect of salts.] Arch Exp Pathol Pharmakol 24 (1888) 247-260.

[47] Y. Zhang, P.S. Cremer, Interactions between macromolecules and ions: the Hofmeister series, Curr Opin in Chemical Biology 10 (2006) 658–663.

[48] W. Kunz, J. Henle, B.W. Ninham, Zur Lehre von der Wirkung der Salze [Title translation: About the science of the effect of salts.]: Franz Hofmeister's historical papers, Curr Opin Colloid Interface Sci 9 (2004) 19-37.

[49] J.N. Sachs, T.B. Woolf, Understanding the Hofmeister effect in interactions between chaotropic anions and lipid bilayers: molecular dynamics simulations. J Am Chem Soc 125 (2003) 8742-8743.

[50] B. Schnell, R. Schurhammer, G. Wipff, Distribution of hydrophobic ions and their counterions at an aqueous liquid-liquid interface: a molecular dynamics investigation, J Phys Chem B 108 (2004) 2285-2294.

[51] K.D. Collins, M.W. Washabaugh, The Hofmeister effect and the behavior of water at interfaces, Q Rev Biophys 18 (1985) 323-422.

[52] A. Labena, M.A. Hegazy, H. Horn, E. Müller, Cationic gemini surfactant as a corrosion inhibitor and a biocide for high salinity sulfidogenic bacteria originating from an oil-field water tank, J. Surfact. Deterg. 17(2014) 419-431.

[53] M. J. Rosen, Surfactants and Interfacial Phenomena, 3rd Ed., John Wiley & Sons, Inc., Hoboken, New Jersey (2004) pp. 63.

[54] M.J. Rosen, Surfactants and Interfacial Phenomena, 2nd Ed., John Wiley and Sons Inc., New York (1989).

[55] A. Labena, M.A. Hegazy, H. Horn, E. Müller, The biocidal effect of a novel synthesized gemini surfactant on environmental sulfidogenic bacteria: planktonic cells and biofilms, Mater. Sci. and Eng.: C 47 (2015) 367–375.

[56] M.J. Rosen, J.T. Kunjappu, Surfactants and Interfacial Phenomena (4th ed.) Hoboken, New Jersey: John Wiley & Sons, 2012, p. 1.

Caption of Figures

Fig. 1. Preparation of the novel cationic surfactant.

Fig. 2. Preparation of the novel gimini surfactant.

Fig. 3. FTIR spectrum of (Z)-2-((pyridin-2-ylimino)methyl)phenol.

Fig. 4. Mass spectrum of (Z)-2-((pyridin-2-ylimino)methyl)phenol.

Fig. 5. ^{1}HNMR spectrum of (Z)-1-dodecyl-2-(2-hydroxybenzylideneamino)pyridinium bromide.

Fig. 6. Mass spectrum of N,N'-(pentane-1,5-diylidene)dipyridin-2-amine.

Fig. 7. ^{1}HNMR spectrum of 2,2'-(pentane-1,5-diylidenebis(azan-1-yl-1-ylidene))bis(1-dodecylpyridinium bromide).

Fig. 8. Nyquist plots for carbon steel in 0.5 M H_2SO_4 in absence and presence of different concentrations of the synthesized cationic and gemini surfactants.

Fig. 9. Suggested equivalent circuit model for the studied systems.

Fig. 10. Bode and Phase angle plots for carbon steel in 0.5 M H_2SO_4 in absence and presence of different concentrations of the synthesized cationic and gemini surfactants.

Fig. 11. Anodic and cathodic polarization curves obtained at 20 ^{o}C in 0.5 M H_2SO_4 in different concentrations of the synthesized cationic and gemini surfactants. (1) 0.5 M H_2SO_4, (2) 1×10^{-4} M, (3) 5×10^{-4} M, (4) 1×10^{-3} M, (5) 5×10^{-3} M and (6) 1×10^{-2} M.

Table 1

Gravimetric results for carbon steel 0.5 M H_2SO_4 without and with different concentrations of the synthesized surfactants at various temperatures

Temp. (^oC)	Inhibitor conc. (M)	Inhibitor name							
		Cationic				Gemini			
		ΔW (mg)	k (mg cm^{-2} h^{-1})	Θ	η_w (%)	ΔW (mg)	k (mg cm^{-2} h^{-1})	Θ	η_w (%)
20	0.00	1171.8 ± 1.15	0.9597	-	-	1171.8 ± 1.15	0.9597	-	-
	1×10^{-4}	491.1 ± 0.63	0.4022	0.58	58.09	380.1 ± 0.55	0.3113	0.68	67.56
	5×10^{-4}	260.2 ± 0.45	0.2131	0.78	77.79	241.1 ± 0.45	0.1975	0.79	79.42
	1×10^{-3}	177.0 ± 0.61	0.1450	0.85	84.90	130.7 ± 0.88	0.1070	0.89	88.85
	5×10^{-3}	118.0 ± 0.44	0.0966	0.90	89.93	95.2 ± 0.67	0.0780	0.92	91.88
	1×10^{-2}	71.2 ± 0.37	0.0583	0.94	93.92	40.3 ± 0.39	0.0330	0.97	96.56
40	0.00	2963.3 ± 1.54	2.4269	-	-	2963.3 ± 1.54	2.4269	-	-
	1×10^{-4}	1341.3 ± 0.72	1.0985	0.55	54.74	770.9 ± 0.77	0.6314	0.74	73.99
	5×10^{-4}	720.7 ± 0.67	0.5903	0.76	75.68	420.8 ± 0.64	0.3446	0.86	85.80
	1×10^{-3}	510.5 ± 0.81	0.4181	0.83	82.77	211.1 ± 0.81	0.1729	0.93	92.88
	5×10^{-3}	320.8 ± 0.77	0.2627	0.89	89.17	151.2 ± 0.66	0.1238	0.95	94.90
	1×10^{-2}	244.2 ± 0.55	0.2000	0.92	91.76	60.6 ± 0.51	0.0496	0.98	97.95
60	0.00	6615.2 ± 1.89	5.4179	-	-	6615.2 ± 1.89	5.4179	-	-
	1×10^{-4}	3121.6 ± 1.11	2.5566	0.53	52.81	1410.0 ± 1.02	1.1548	0.79	78.69
	5×10^{-4}	1731.4 ± 0.94	1.4180	0.74	73.83	671.7 ± 0.83	0.5501	0.90	89.85
	1×10^{-3}	1210.9 ± 0.85	0.9917	0.82	81.70	321.6 ± 0.68	0.2634	0.95	95.14
	5×10^{-3}	880.6 ± 0.55	0.7212	0.87	86.69	242.0 ± 0.72	0.1982	0.96	96.34
	1×10^{-2}	660.5 ± 0.62	0.5410	0.90	90.02	80.9 ± 0.56	0.0663	0.99	98.78

Table 2

Electrochemical parameters of impedance for carbon steel in 0.5 M H_2SO_4 without and with different concentrations of the synthesized surfactants at 20 ^oC

Inhibitor name	Inhibitor conc. (M)	R_s (Ω cm²)	R_{ct} (Ω cm²)	Q			C_{dl} (μF cm^{-2})	η_I
				Y_o (μF cm^{-2})	n	Error of n (%)		
	0.00	1.4	62 ± 1.3	1.49	0.98	0.23	91.8	-
Cationic	1×10^{-4}	1.5	155 ± 1.2	0.60	0.96	0.42	36.8	59.9
	5×10^{-4}	1.6	276 ± 1.1	0.36	0.88	1.39	21.7	77.5
	1×10^{-3}	1.7	413 ± 1.9	0.25	0.90	1.33	14.1	85.1
	5×10^{-3}	1.9	688 ± 1.7	0.12	0.94	0.74	8.3	91.0
	1×10^{-2}	2.4	1075 ± 2.1	0.07	0.79	1.45	5.2	94.2
Gemini	1×10^{-4}	1.6	198 ± 1.5	0.48	0.97	0.53	29.8	67.5
	5×10^{-4}	1.8	325 ± 1.8	0.27	0.92	1.34	17.5	80.7
	1×10^{-3}	2.1	559 ± 0.9	0.21	0.91	146	10.3	88.9
	5×10^{-3}	2.4	730 ± 2.2	0.11	0.95	1.26	7.8	91.5
	1×10^{-2}	2.7	1212 ± 2.5	0.06	0.81	2.34	4.5	94.9

Table 3

Potentiodynamic polarization results for carbon steel in 0.5 M H_2SO_4 without and with different concentrations of the synthesized surfactants at 20 ^oC

Inhibitor name	Inhibitor conc. (M)	E_{corr} (mV(SCE))	i_{corr} (mA cm^{-2})	β_a (mV dec^{-1})	β_c (mV dec^{-1})	η_p (%)
	0.00	-502	0.2889 ± 0.0019	121	-168	-
Cationic	1×10^{-4}	-502	0.1151 ± 0.0021	129	-174	60.2
	5×10^{-4}	-505	0.0668 ± 0.0015	178	-136	76.9
	1×10^{-3}	-509	0.0418 ± 0.0013	168	-185	85.5
	5×10^{-3}	-513	0.0279 ± 0.0017	157	-116	90.3
	1×10^{-2}	-523	0.0168 ± 0.0011	106	-170	94.2
Gemini	1×10^{-4}	-502	0.0920 ± 0.0018	149	-168	67.5
	5×10^{-4}	-505	0.0638 ± 0.0013	161	-136	79.5
	1×10^{-3}	-507	0.0322 ± 0.0017	139	-182	88.9
	5×10^{-3}	-512	0.0240 ± 0.0014	188	-119	91.9
	1×10^{-2}	-520	0.0011 ± 0.0007	119	-166	96.6

Table 4

The thermodynamic parameters of adsorption of the synthesized surfactants at different concentrations for carbon steel in 0.5 M H_2SO_4 solution

Inhibitor name	Temp. (^oC)	Slope	Intercept	R^2	K_{ads} (M^{-1})	ΔG^o_{ads} (kJ mol^{-1})	ΔH^o_{ads} (kJ mol^{-1})	ΔS^o_{ads} (J mol^{-1} K^{-1})
Cationic	20	1.05	0.0001170	0.9998	8547	-31.84	-1.90	102.19
	40	1.08	0.0001202	0.9999	8319	-33.94		102.38
	60	1.10	0.0001286	0.9998	7776	-35.92		102.18
Gemini	20	1.03	0.0001124	0.9994	8897	-31.94	15.66	162.43
	40	1.01	0.0000726	0.9998	13774	-35.25		162.65
	60	1.01	0.0000520	0.9999	19231	-38.43		162.42

Table 5

Surface properties of the synthesized cationic and gemini surfactants from surface tension and conductivity measurements at 20 ^{o}C

Inhibitor name	Solvent	Surface tension measurements					Conductivity measurements		
		$C_{cmc} \times 10^3$ (mol dm^{-3})	γ_{cmc} (mN m^{-1})	π_{cmc} (mN m^{-1})	$\Gamma_{max} \times 10^{10}$ (mol cm^{-2})	A_{min} (nm^2)	$C_{cmc} \times 10^3$ (mol dm^{-3})	β	ΔG^{o}_{m} (kJ mol^{-1})
Cationic	Bidistiled water	1.24	27	45	5.70	0.29	1.25	0.31	-27.61
Gemini		0.88	24.5	47.5	9.89	0.17	0.87	0.34	-28.46
Cationic	0.5 M H_2SO_4	1.13	29	43	5.66	0.30	-	-	-
Gemini		0.77	27	45	6.32	0.26	-	-	-

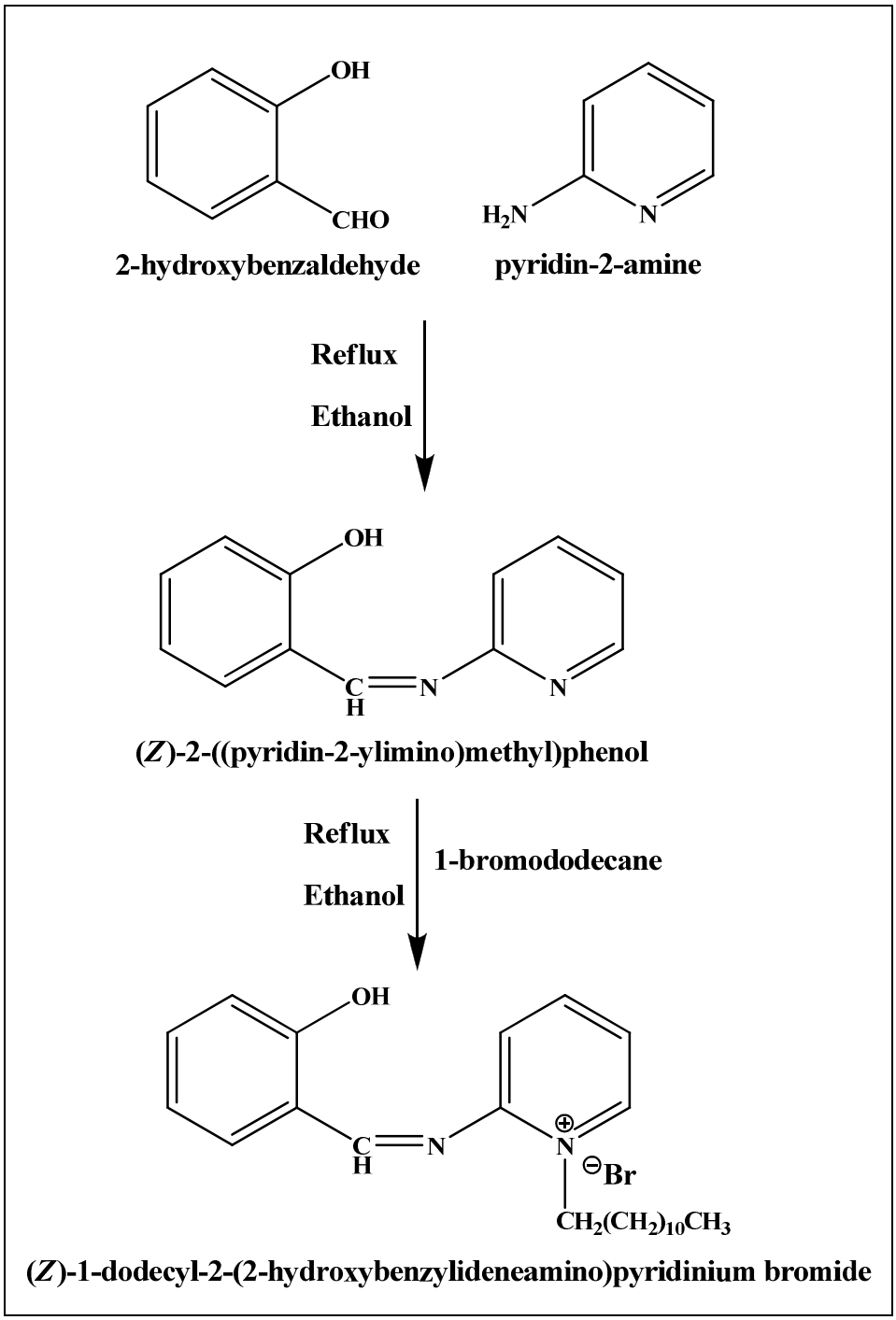

Fig. 1

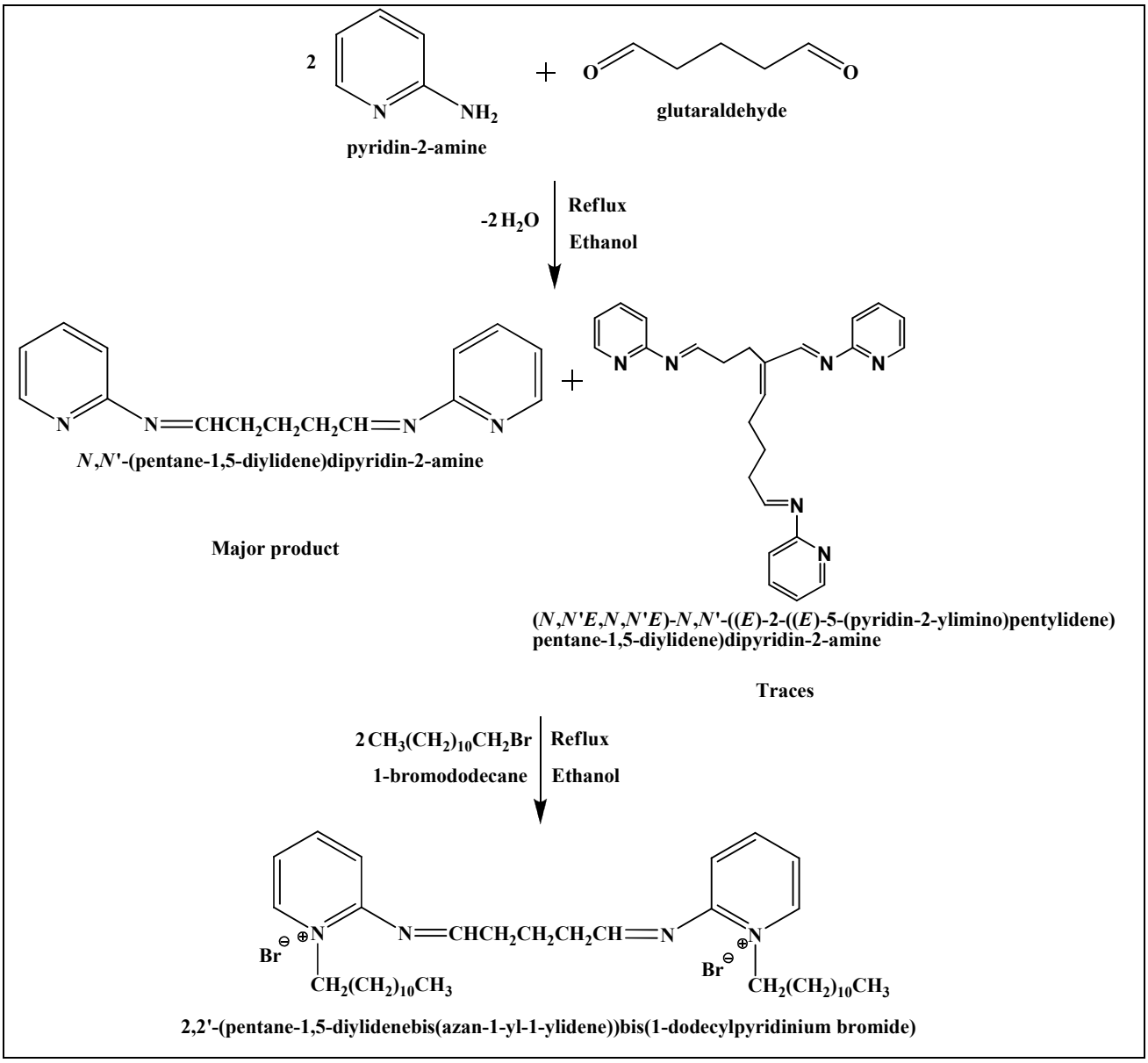

Fig. 2

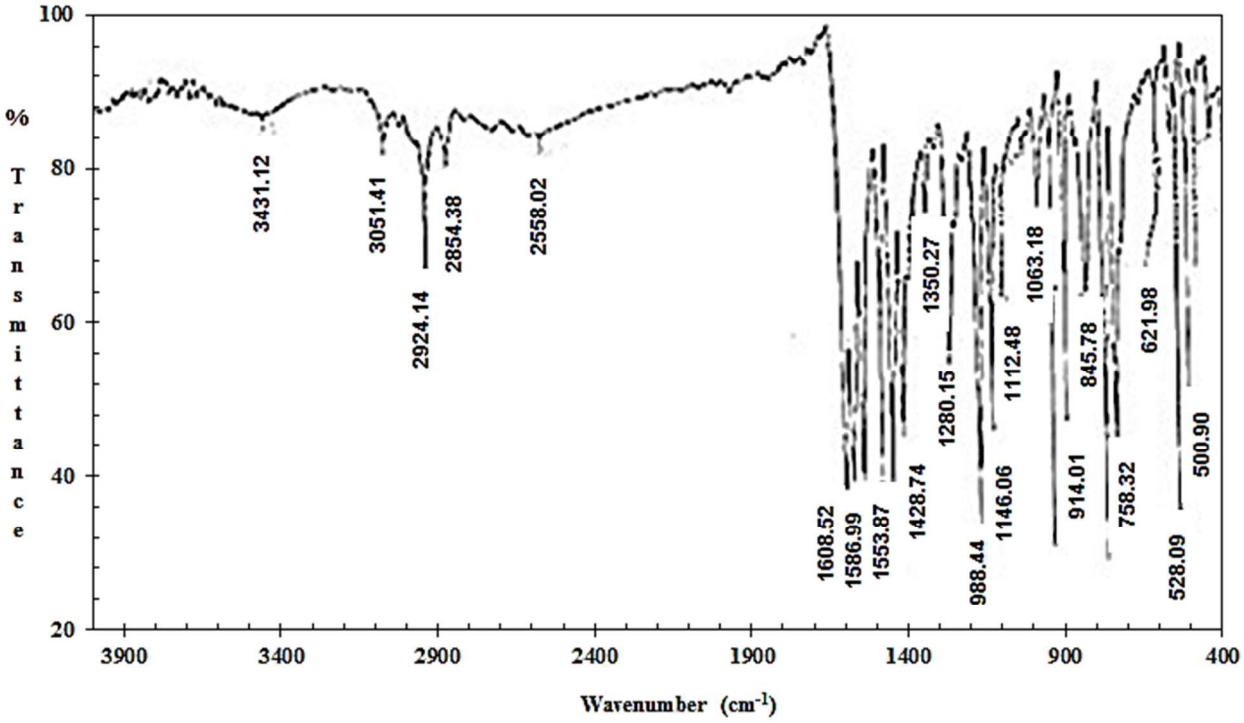

Fig. 3

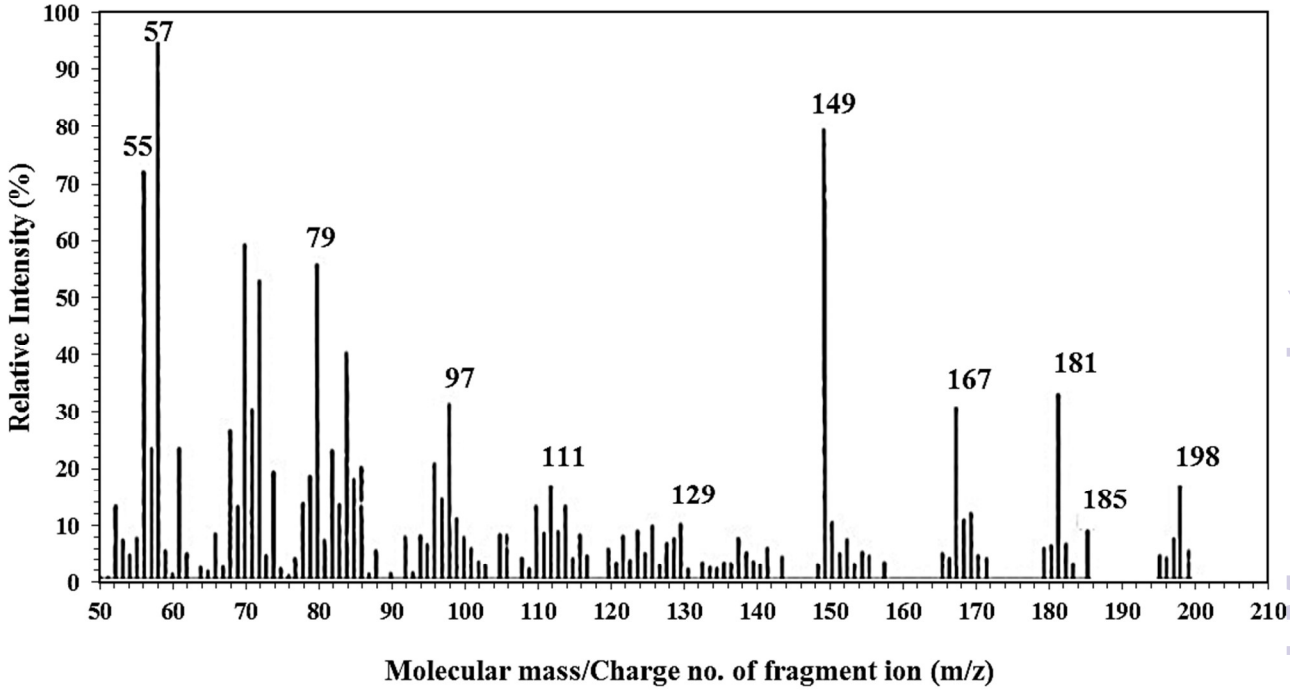

Fig. 4

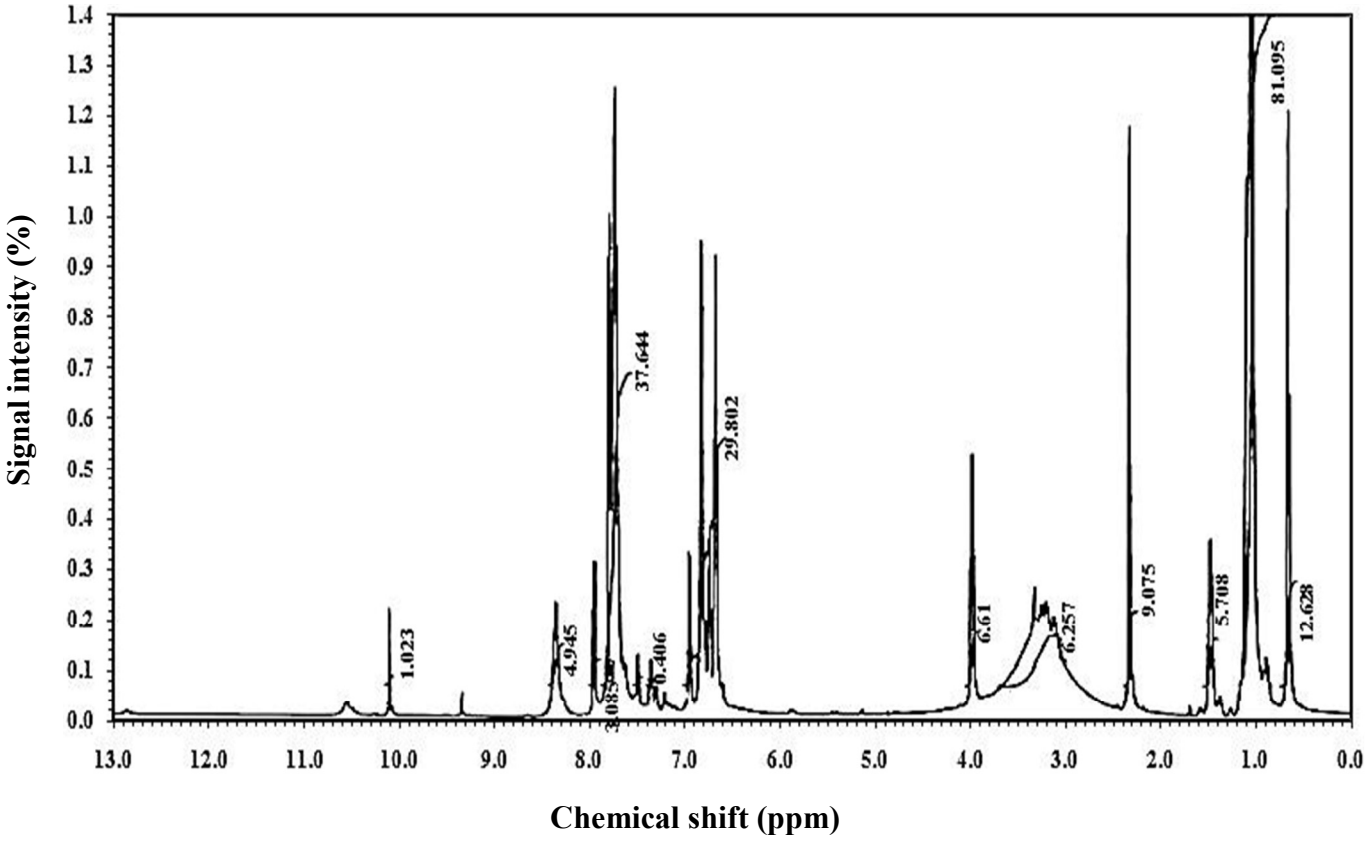

Fig. 5

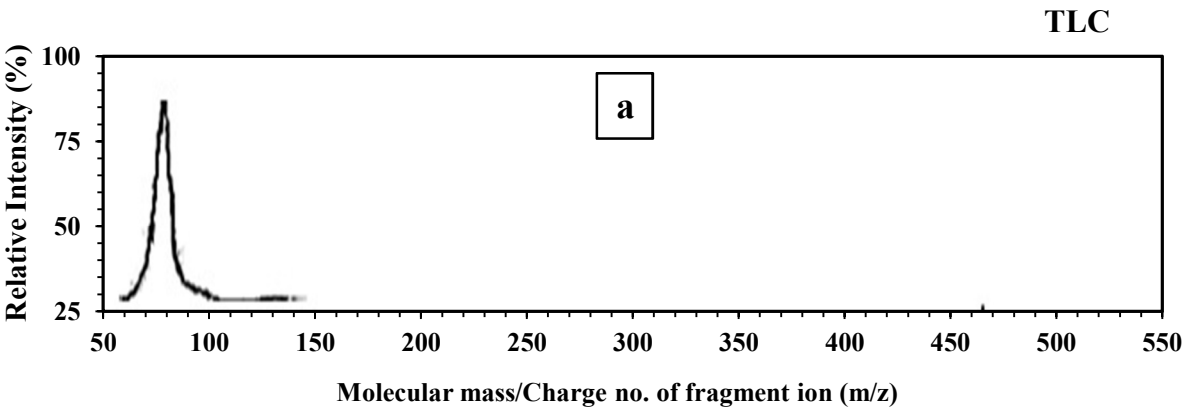

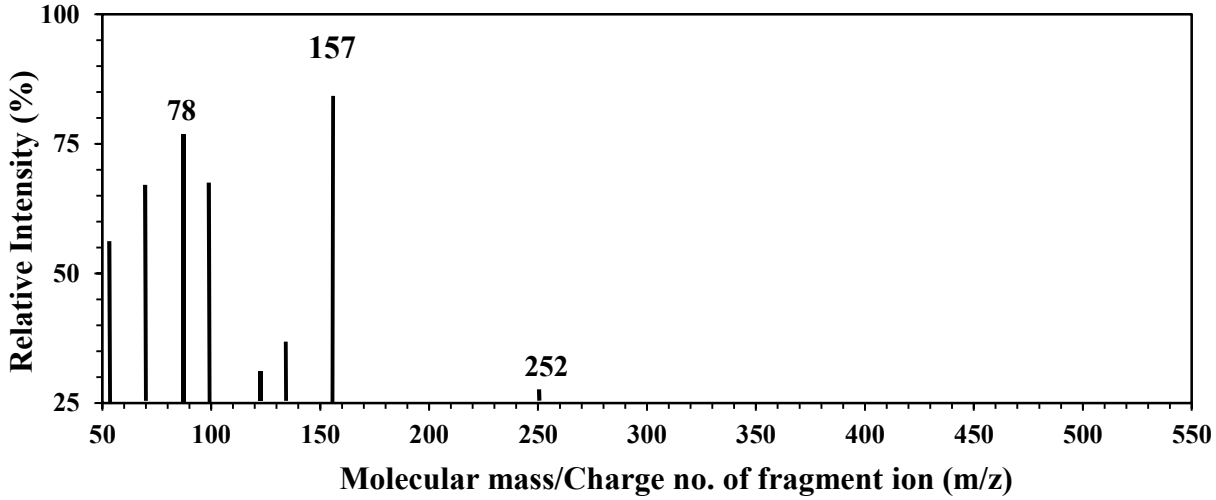

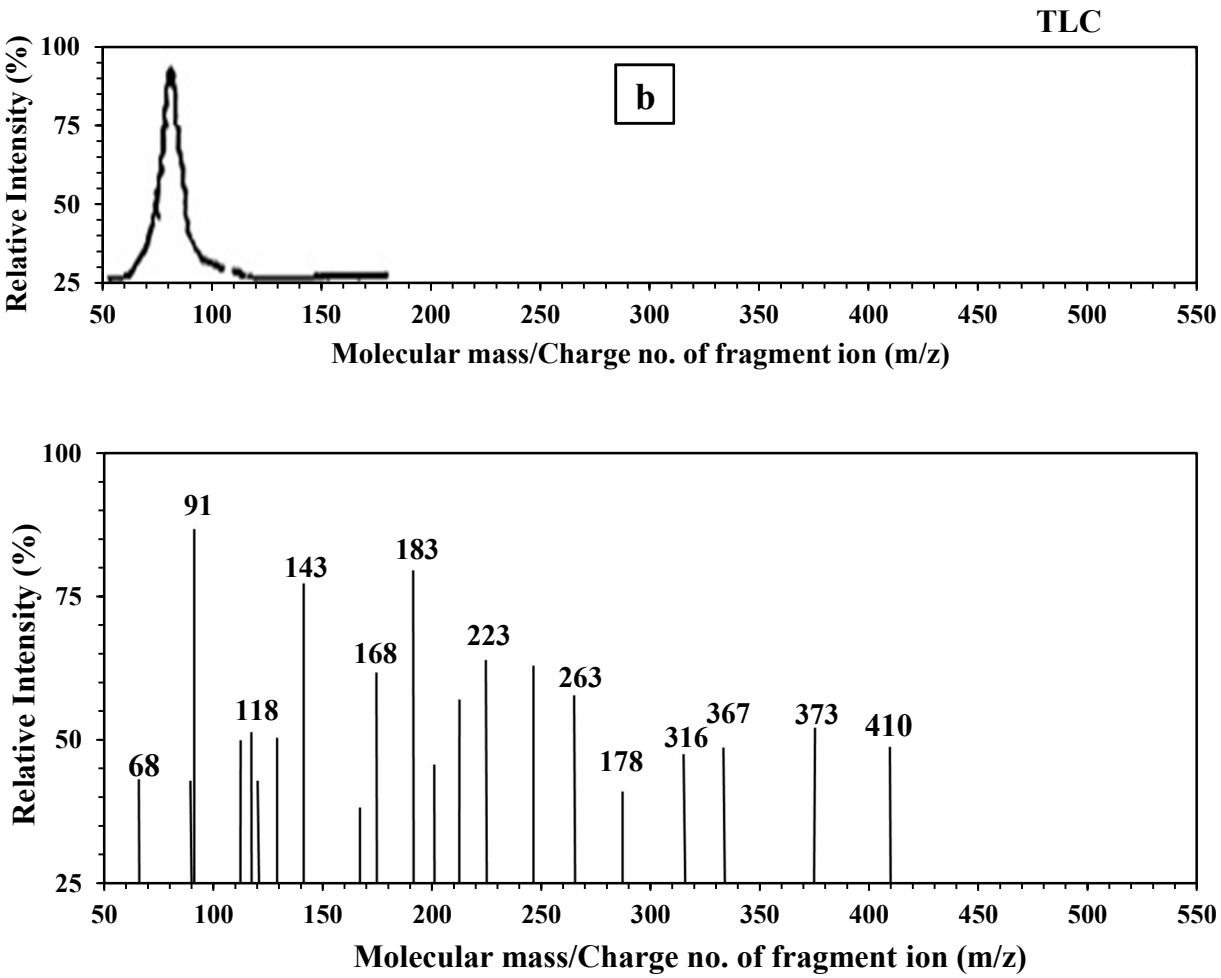

Fig. 6

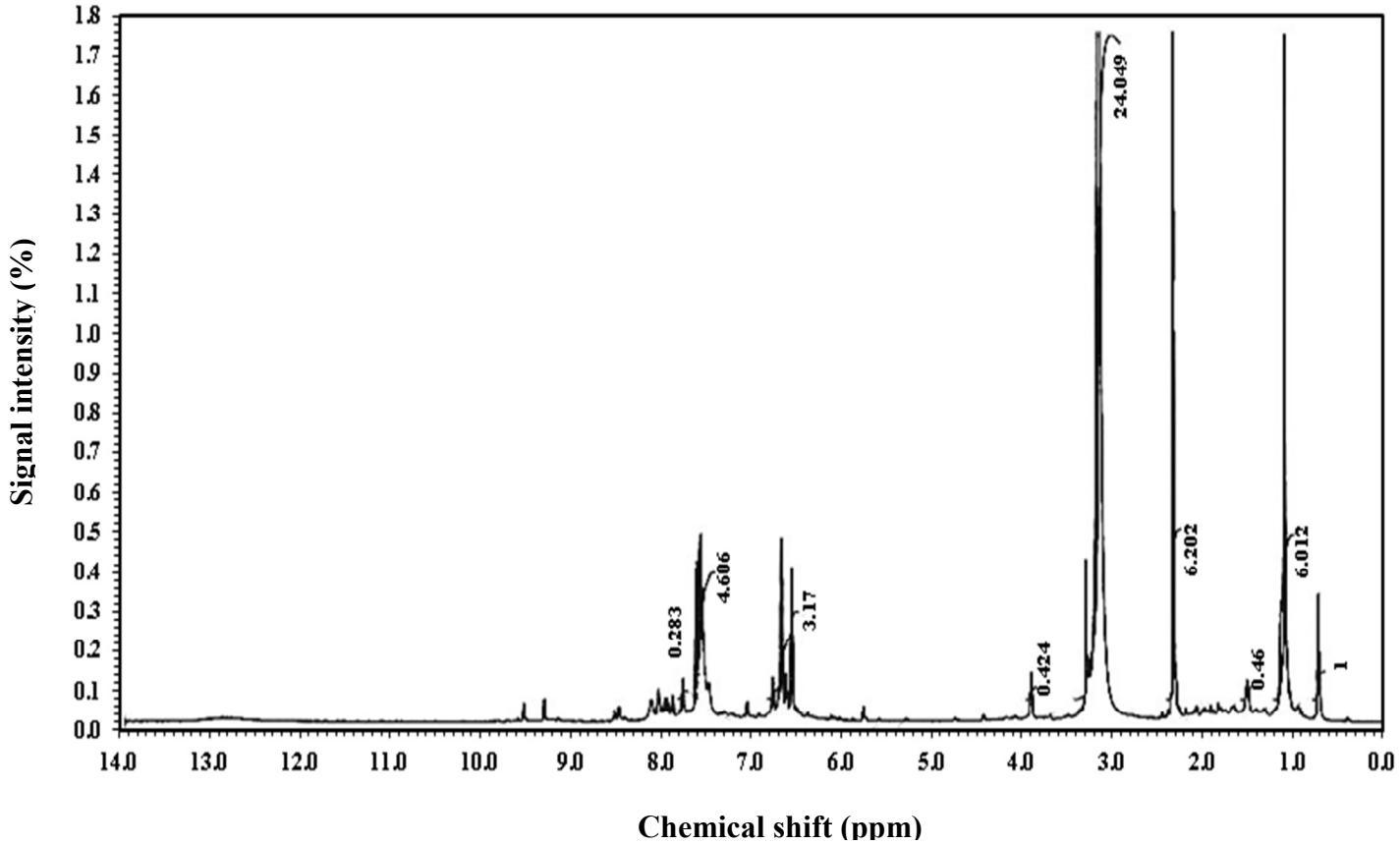

Fig. 7

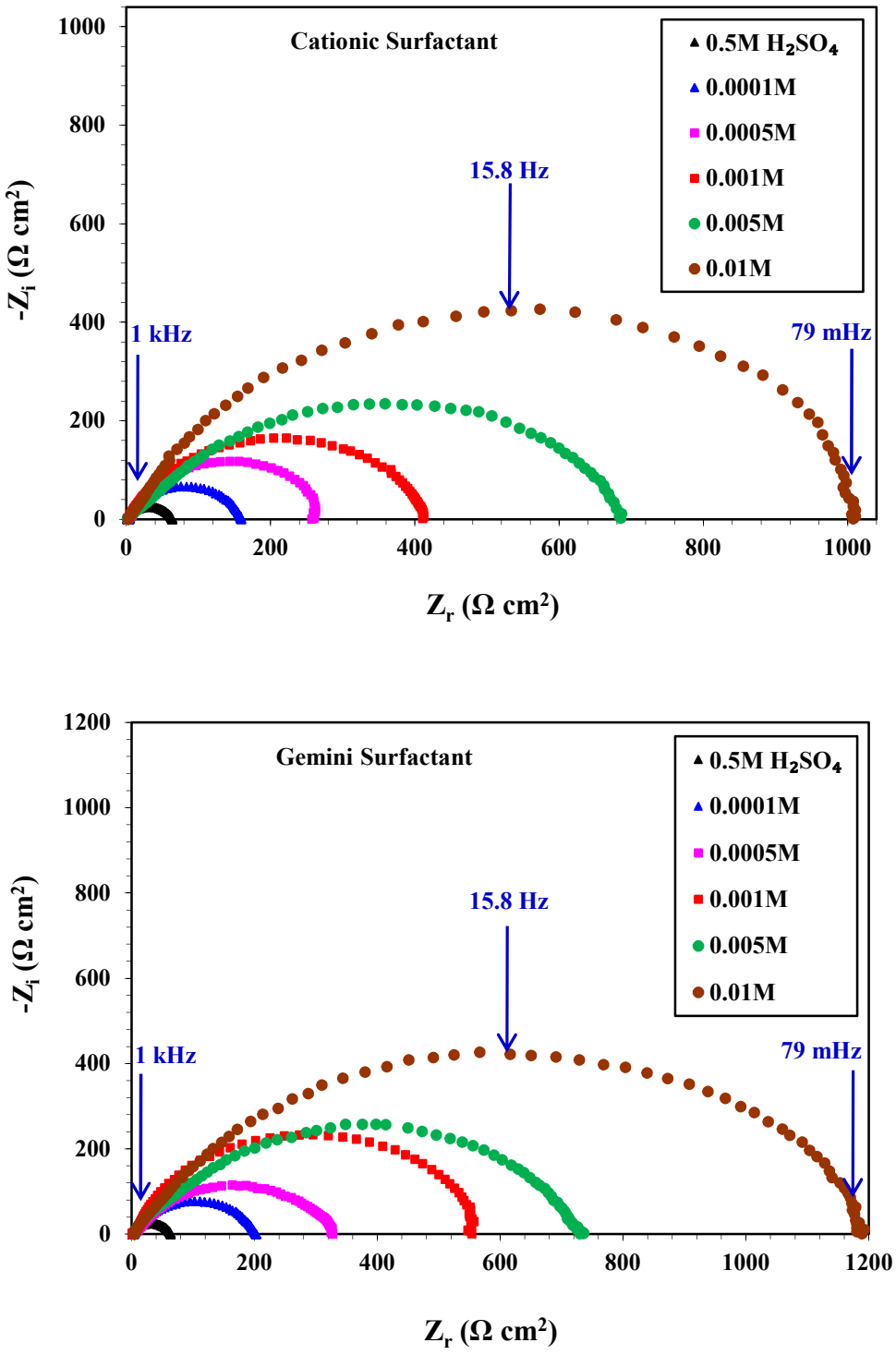

Fig. 8

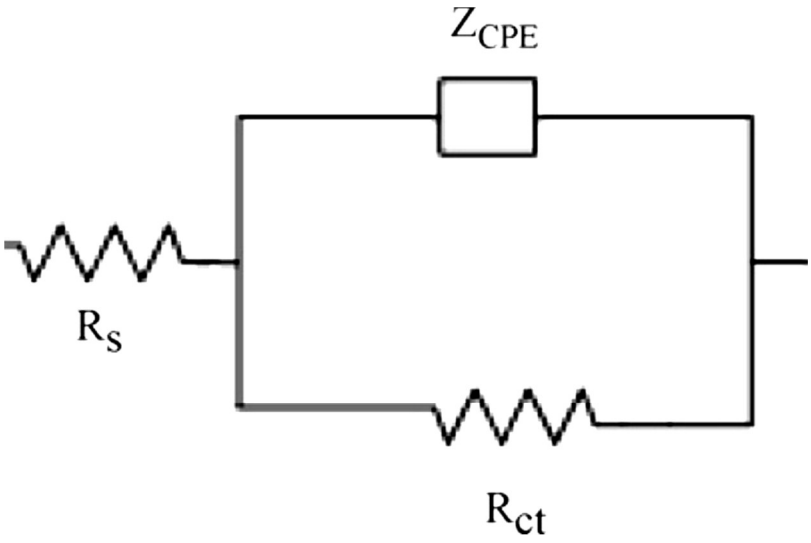

Fig. 9

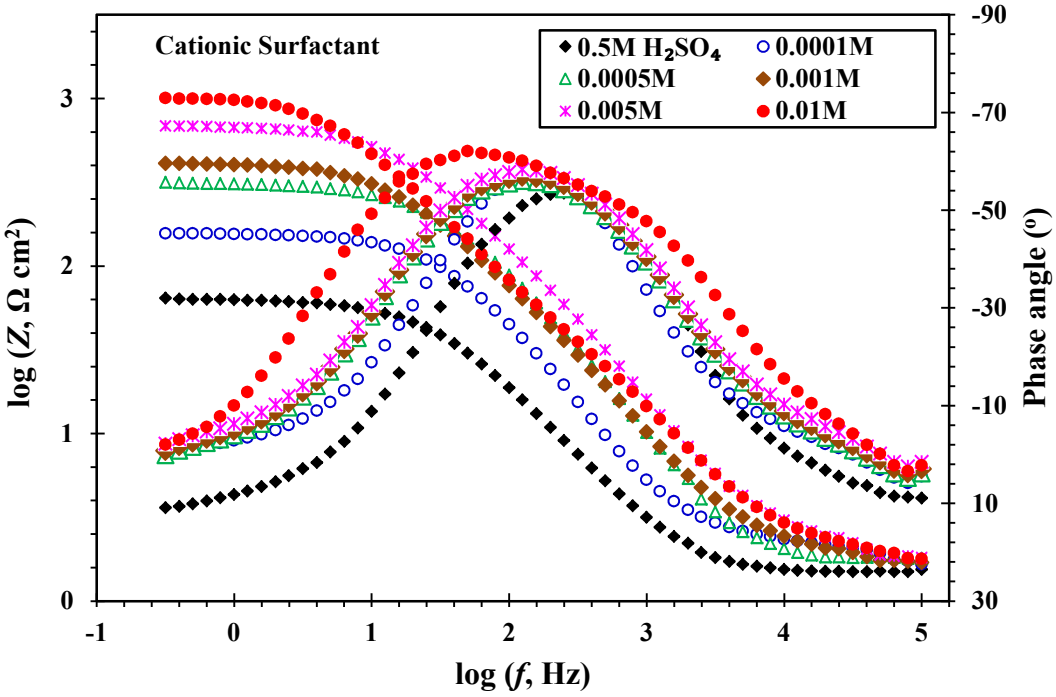

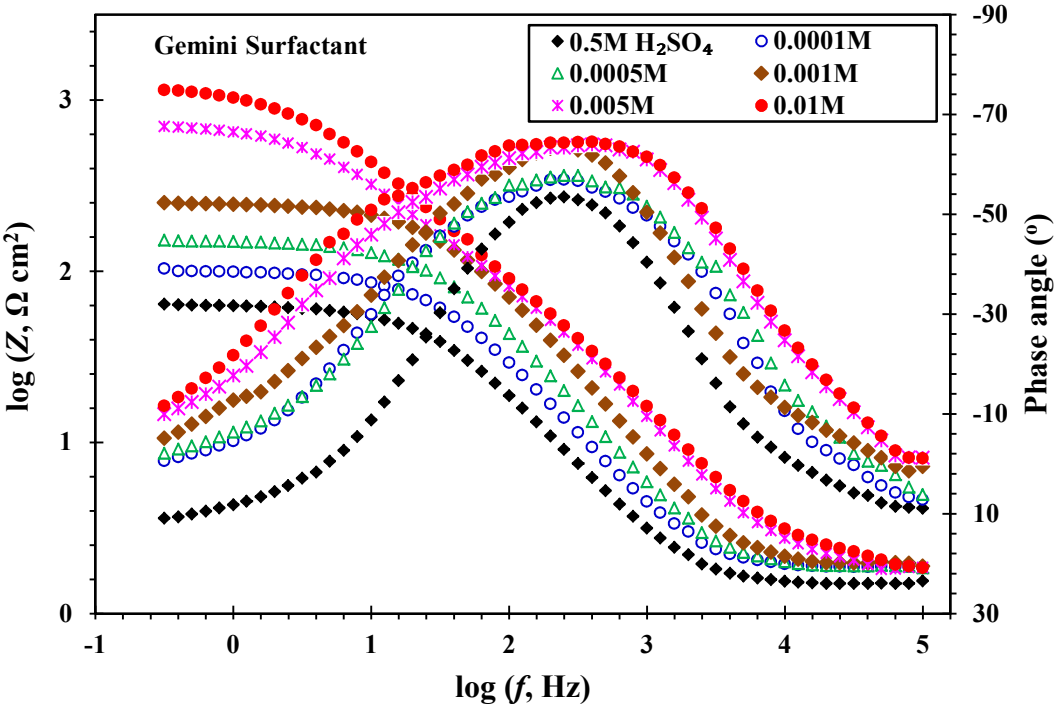

Fig. 10

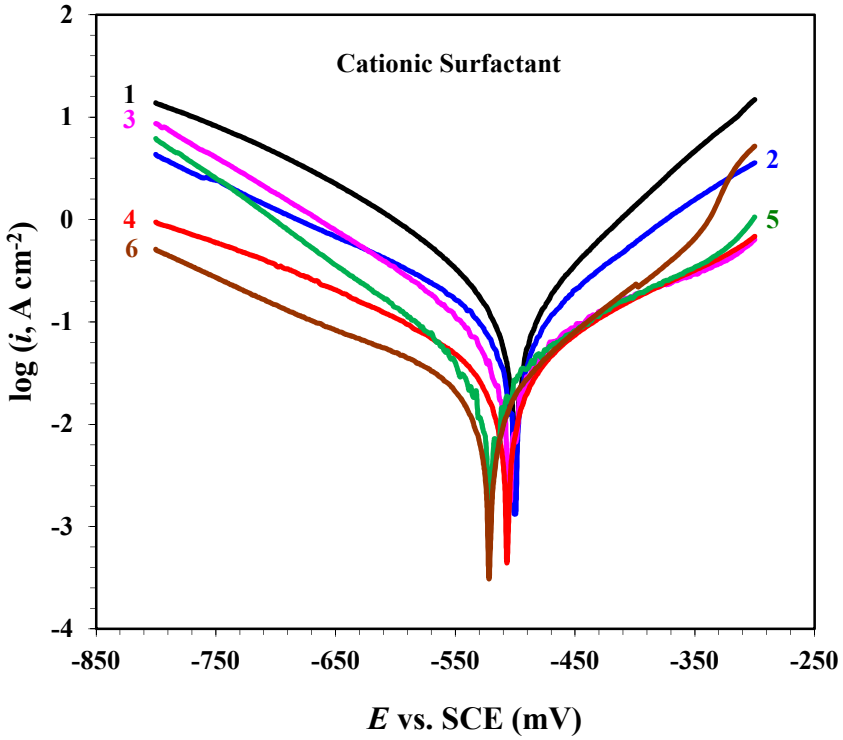

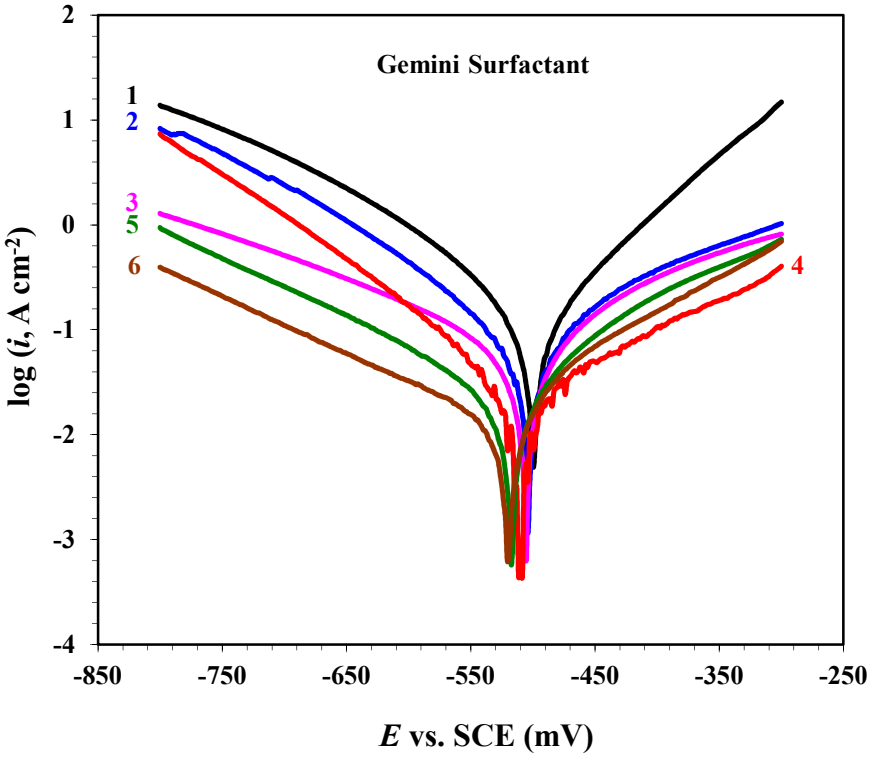

Fig. 11

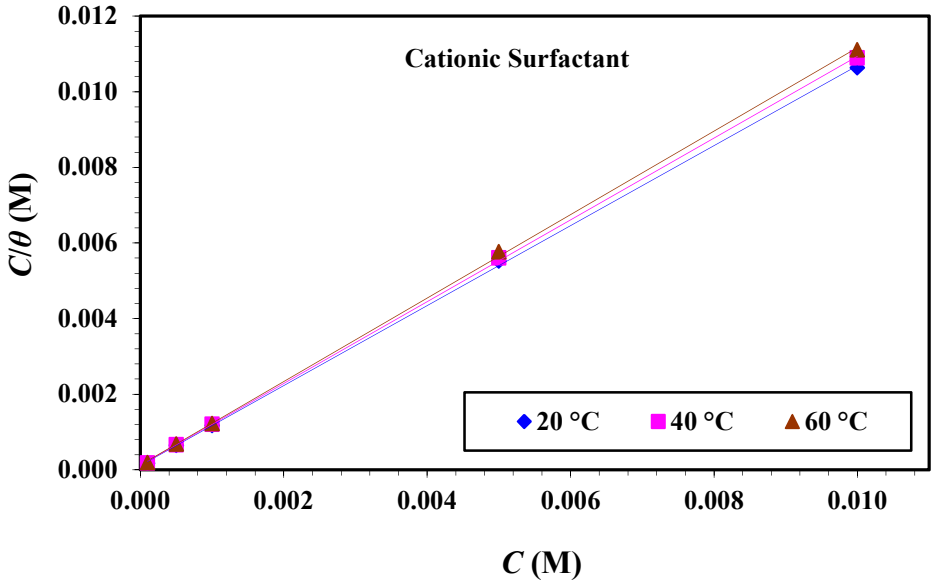

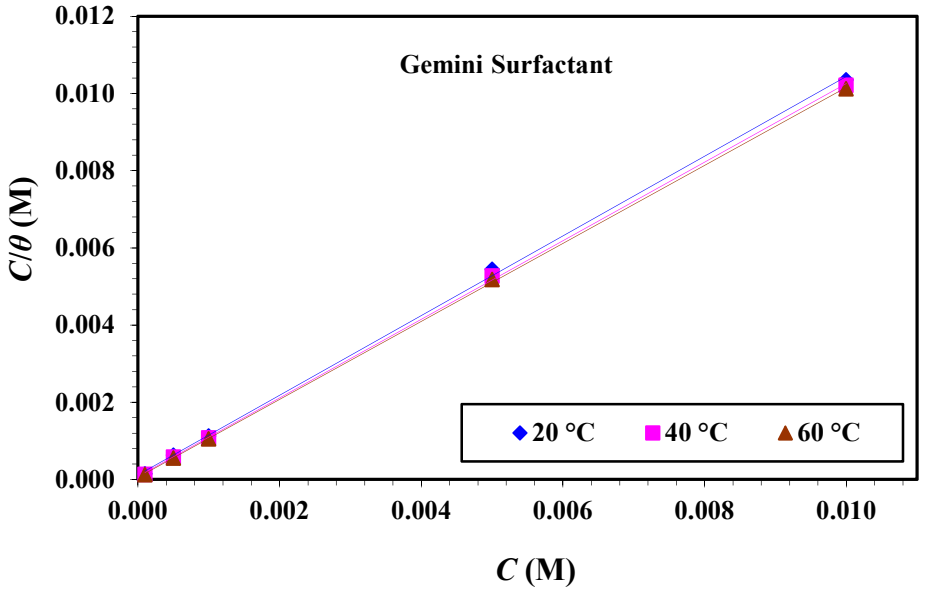

Fig. 12

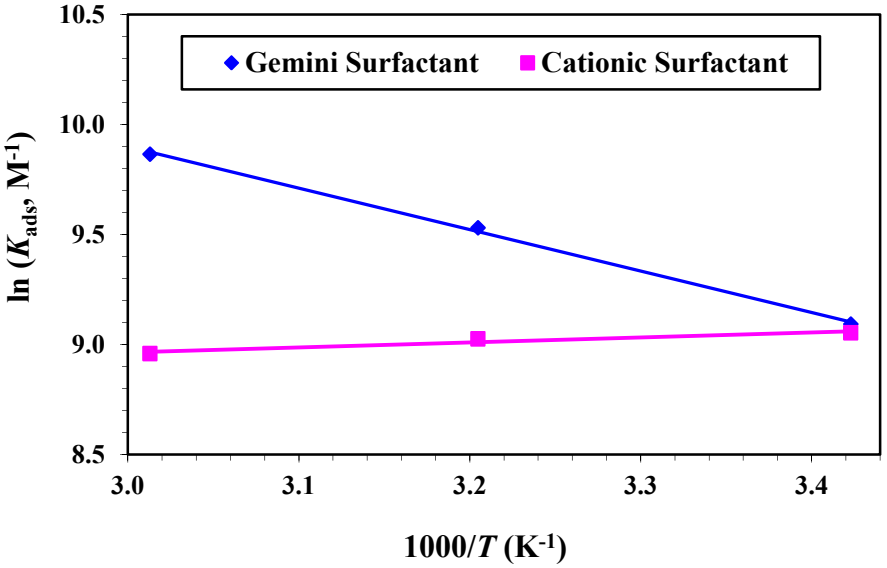

Fig. 13

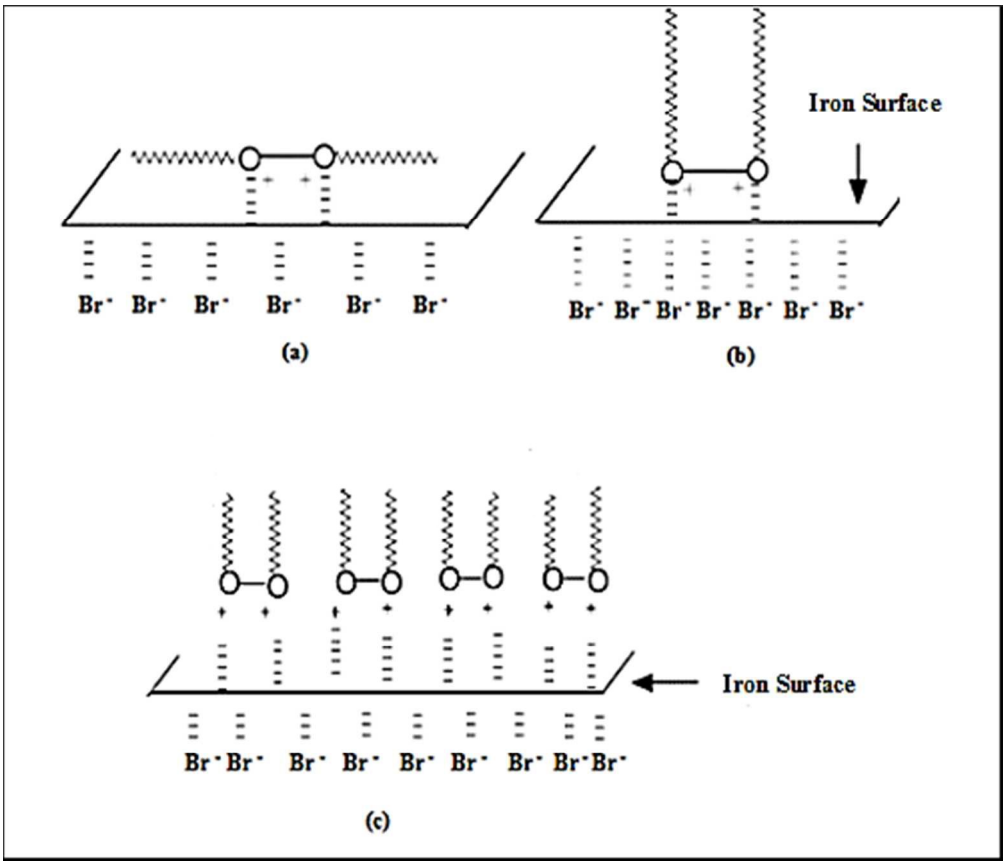

Fig. 14

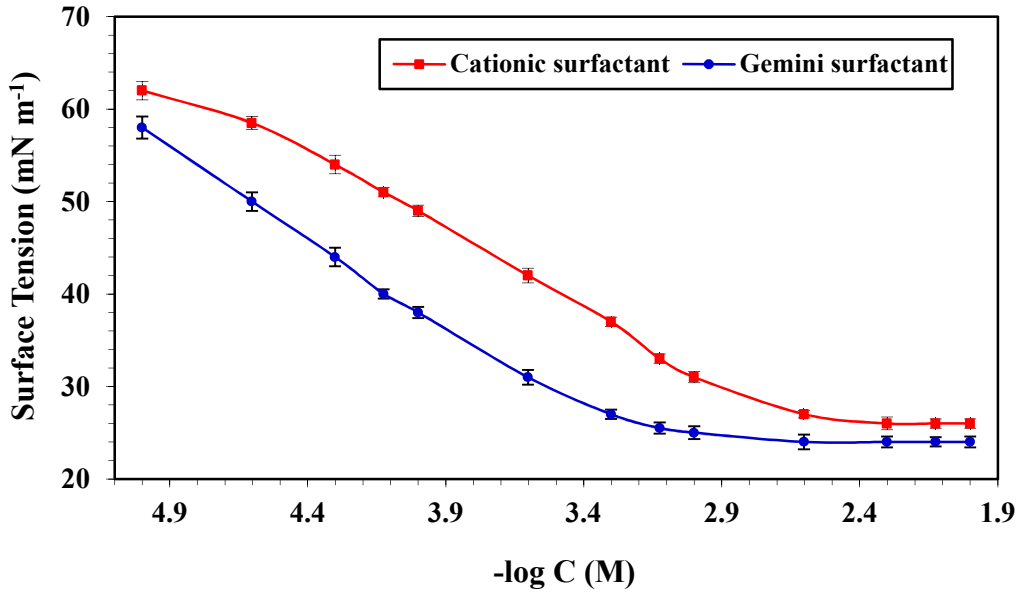

Fig. 15

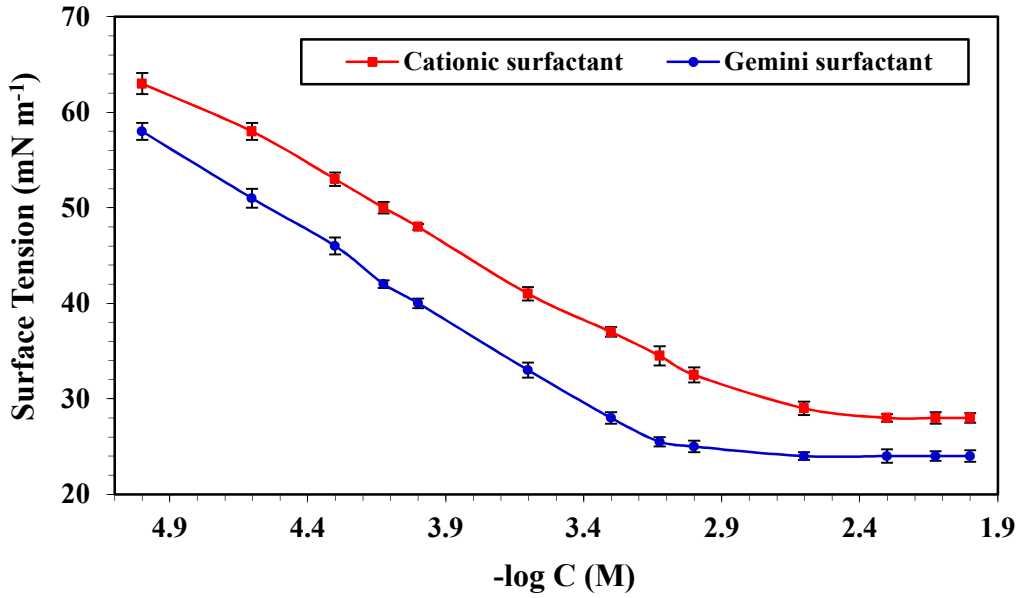

Fig. 16

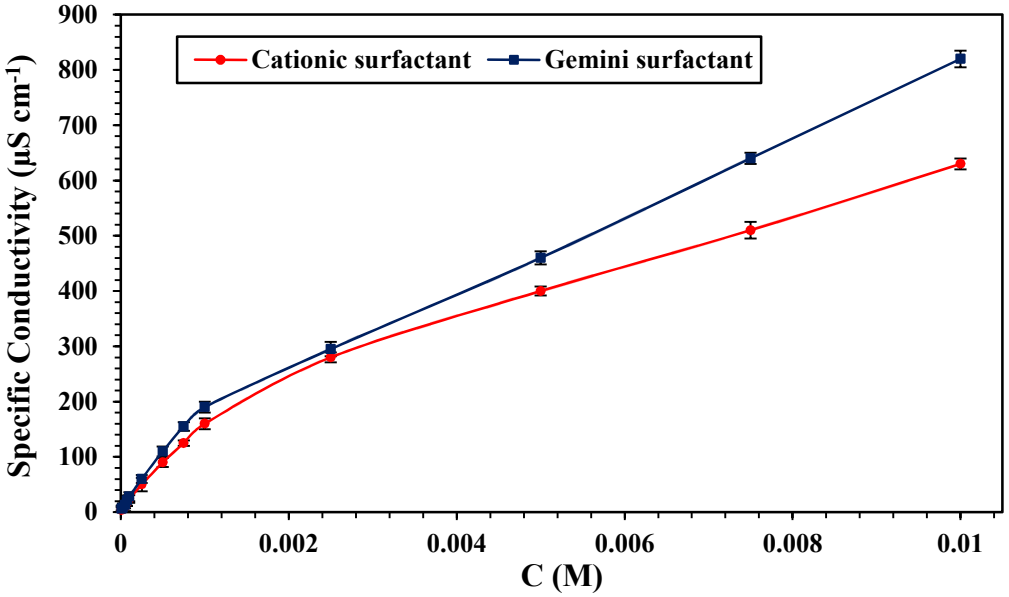

Fig. 17

Graphical abstract